JUNE 2023

M.Sc. in ENGINEERING PHYSICS

HATİCE ŞABRAK

REPUBLIC OF TÜRKİYE

GAZİANTEP UNIVERSITY

GRADUATE SCHOOL OF NATURAL & APPLIED SCIENCES

HEAVY-ION FUSION REACTIONS AT EXTREME SUB-BARRIER ENERGIES

M.Sc. THESIS

IN

ENGINEERING PHYSICS

BY

HATİCE ŞABRAK

JUNE 2023

HEAVY-ION FUSION REACTIONS AT EXTREME SUB-BARRIER ENERGIES

M.Sc. Thesis

in

Engineering Physics

Gaziantep University

Supervisor

Prof. Dr. Bülent GÖNÜL

by

Hatice ŞABRAK

June 2023

I hereby declare that all information in this document has been obtained and presented in accordance with academic rules and ethical conduct. I also declare that, as required by these rules and conduct, I have fully cited and referenced all material and results that are not original to this work.

Hatice ŞABRAK

ABSTRACT

HEAVY-ION FUSION REACTIONS AT EXTREME SUB-BARRIER ENERGIES

ŞABRAK, Hatice
M.Sc. in Engineering Physics
Supervisor: Prof. Dr. Bülent GÖNÜL

June 2023

55 pages

Recent years have witnessed an increase in interest in the study of fusion reactions at extreme sub-barrier energies, despite the fact that it is challenging to measure them due to their extremely small cross sections. Such reactions are essential to understand the creation of heavy elements in varied settings. In the present thesis work, the status of the field is reviewed involving all the related theoretical and experimental works carried out so far. The unexpected behavior seen in the steep falloff of measured cross-sections at low incident energies is explained in detail using new physics concepts related to the fusion process of atomic nuclei. Besides that, the framework of the sudden and adiabatic approaches using different potential structures especially shallow and deep potentials is discussed through the supersymmetric phase equivalent potential concept in quantum theory.

Key Words: Heavy-ion Reactions, Extreme Sub-barrier Energies, Fusion Hindrance.

ÖZET

BARIYER ALTI AŞIRI DÜŞÜK ENERJILI AĞIR-IYON FÜZYON REAKSIYONLARI

ŞABRAK, Hatice
Yüksek Lisans, Fizik Mühendisliği
Danışman: Prof. Dr. Bülent GÖNÜL

Haziran 2023

55 sayfa

Çok küçük sayısal değerlere sahip reaksiyon tesir kesitlerinde ölçüm zorluklarına rağmen, yakın zamanda düşük enerjili füzyon reaksiyonlarıyla ilgili çalışmalarda artış gözlemlenmiştir. İlgilenilen reaksiyonlar, farklı ortamlarda mevcut ağır elementlerin üretimi konusunu anlayabilmemiz açısından oldukça önem arz etmektedir. Bu tez çalışmasında, söz konusu alanda günümüze değin yürütülen tüm teorik ve deneysel çalışmalar gözden geçirilmiştir. Bahse konu düşük enerjilerde, ağır atom çekirdeklerinin füzyon dinamiğini açıklayan ilgili reaksiyon tesir kesitlerinde gözlemlenen ve teorik olarak beklenmeyen ani düşüşlere getirilen fiziksel tabanlı açıklamalar, yeni kuramsal fizik tartışmaları ışığında dikkatle incelendi. Ek olarak; tamamen farklı yapılarda sığ ve derin potansiyel fonksiyonlar içeren ve ilgili literatürde Ani/Sudden ve Yavaş/Adiabatic yaklaşımlar olarak bilinen iki farklı kuramsal modelin söz konusu reaksiyonlarda başarıyla benzer sonuçlar üretmesi, süpersimetrik kuantum mekaniği çerçevesinde faz eşdeğerli sığ ve derin potansiyel kavramı göz önünde bulundurularak tartışılmış ve gerekli fiziksel tabanlı izahat verilmiştir.

Anahtar Kelimeler: Ağır-iyon Reaksiyonları, Bariyer Altı Aşırı Düşük Enerjiler, Füzyon Engeli.

"Dedicated to my family"

ACKNOWLEDGEMENTS

I would like to express my sincere gratitude to Prof. Dr. Bülent GÖNÜL for his unwavering support, invaluable guidance, and endless patience throughout the entire duration of this thesis work. His insightful feedback and constructive criticism have been instrumental in shaping my research and enhancing the quality of this thesis.

I am also deeply grateful to all the academicians whose expertise and constructive feedback have greatly contributed to my development throughout my master's degree journey.

Lastly, I would like to thank my family, friends, and loved ones for their endless support, encouragement, and understanding, without which this accomplishment would not have been possible.

TABLE OF CONTENT

ABSTRACT ..... **vi**
ÖZET ..... **viii**
ACKNOWLEDGEMENTS ..... **viii**
TABLE OF CONTENT ..... **ix**
LIST OF FIGURES ..... **x**
CHAPTER 1 INTRODUCTION **1**
CHAPTER 2 THEORETICAL BACKGROUND **4**
2.1 Potential model and the Wong formula 7
2.2 Attempts to improve the potential model 9
2.2.1 Channel coupling effect with a repulsive nucleon-nucleon force 11
2.2.2 Test of the shallow nature of the nuclear potential 15
2.2.3 Concluding remarks on these amendments 22
2.3 Discussion on Pauli repulsion 24
CHAPTER 3 DEEP SUB-BARRIER HINDRANCE **28**
3.1 Theoretical models: sudden versus adiabatic 30
3.2 A remark on deep and shallow potentials 34
3.3 Supersymmetry between deep and shallow potentials used by sudden and adiabatic models 35
CONCLUSION **41**
REFERENCES **45**
APPENDIX A THE ION-ION POTENTIAL **48**
APPENDIX B A BREIF DICUSSION ABOUT COUPLED-CHANNELS EQUATIONS **51**
APPENDIX C POTENTIAL DESCRIPTION IN THE ADIABATIC APPROACH **54**
CURRICULUM VITAE **55**

LIST OF FIGURES

Fig.1.1 Fusion cross section for the system ^{64}Ni +^{64}Ni (data: Beckerman [4], Jiang [5]). Illustrating the impacts of hindered fusion and enhanced fusion. 2

Fig.2.1 Description of the internucleus potential between two nuclei in relation to the distance separating them (the solid line). The ^{16}O+^{144}Sm reaction is commonly regarded as a standard instance. The Coulomb and the nuclear components are indicated by the dotted and the dashed lines, respectively. R_b and V_b indicate the Coulomb barrier's position and height, respectively. While Rt_{ouch} refers to the point at which the two nuclei touch each other. 5

Fig.2.2 Potential model calculations for the ^{16}O+^{154}Sm system. 9

Fig.2.3 Different spherical ion-ion potentials for ^{64}Ni + ^{64}Ni. 13

Fig.2.4 Different calculations in comparison to the experimental fusion excitation function for the ^{64}Ni + ^{64}Ni system. 14

Fig.2.5 Observation of the double-folding nuclear potentials (with and without the presen**ce** of repulsion) and the Akyüz-Winter potential for the system ^{64}Ni+^{64}Ni. 18

Fig.2.6 Ion-ion potentials for various systems 19

Fig.2.7 Comparison different treatments of fusion excitation functions for various systems. 19

Fig.2.8 The experimental *S* factors for the different systems in comparison with CC calculations carried out using the M3Y+repulsion and A-W potentials. .20

Fig.2.9 Logarithmic derivatives of the energy weighted cross sections for several heavy-ion interactions**.....**21

Fig.2.10 Assessment of the overall potential produced from the M3Y + Pauli potential (red solid line) with the one gained from the standard M3Y potential (green solid line) for the system α + ^{208}Pb. The Coulomb potential involved is the double-folding potential (black solid line). The Pauli blocking potential, standard M3Y potential, and M3Y + Pauli potential are illustrated by the pink dot line, blue dot line, and black dash line, respectively**.....**26

Fig.3.1 The illustration taken from [1] shows a schematic comparison of the sudden model with the adiabatic model for the hindrance of deep-sub barrier fusion. 29

Fig.3.2 Relationship between incident energy and average angular momentum of the compound nucleus for ^{64}Ni + ^{64}Ni. Quoted from [13]. The M3Y+ repulsive potential was employed to generate the outcomes of the sudden model. **.....**31

Fig.3.3 The upper panel shows the fusion excitation function, while the lower panel displays the astrophysical *S* factor of ^{16}O + ^{208}Pb compared to several CC calculations. Taken from [13]. **.....**33

Fig.3.4 The internuclear potential and the fusion reaction dynamics examined in the sudden and adiabatic models. Taken from Ref. [24]. **.....**34

Fig.A.1 Entrance channel potentials for the fusion of ^{48}Ca + ^{48}Ca. The Woods-Saxon potential (dotted curve) is compared to the M3Y potential with (solid curve) and without (dashed curve) repulsion. The corresponding ground-state energy of the fused system ^{96}Zr is also indicated by the horizontal bar. Taken from [12]**.** **.....**50

Fig.B.1 Fusion cross sections for ^{40}Ca + ^{96}Zr are compared with CC calculations (taken from Ref.[13]). The red line reproducing the data includes couplings to the one- and two-nucleon transfer channels besides the inelastic excitation 2^+ and 3^- of both nuclei**.** **.....**53

CHAPTER 1
INTRODUCTION

Quantum tunneling governs low-energy fusion reactions through the Coulomb barrier which is established due to the termination between the opposing forces that come into play during the collision of nuclei which are the attractive nuclear force at close distances and the repulsive Coulomb barrier at far distances.The study of low-energy fusion interactions between two nuclei, which is the most intricate process, has been subject to extensive research for over 60 years. This research gained additional importance, particularly following the detection of enhanced fusion at sub-barrier energies resulting from the couplings between intrinsic excitations of the two nuclei involved in the reaction. So the sub-barrier fusion reactions of heavy ions provide a great opportunity to understand and explore a fundamental aspect of quantum tunneling when couplings are present. This topic has gained significant attention in various fields of physics and chemistry. Additionally, reactions constructed by heavy ions are crucial for the expansion of the table of elements and the creation of highly massive elements.

Fusion cross sections, which are one of the important experimental observables, have been conducted over an extensive range across twelve arrangements of magnitude, spanning from barn to pb. This range is significantly wider than that for any other nuclear reaction, enabling the observation of behaviors at very deep sub-barrier energies (see recent reviews: [1], and the related references therein).

The advancement of the Coupled-Channels (CC) model was prompted by the discrepancies between the classical formula's predictions and the cross-sections that have been measured at energies near the Coulomb barrier, and it is known as the sub-barrier fusion enhancement phenomenon [2]. To investigate this phenomenon, cross-section measurements as low as 0.1mb were necessary. Similarly, researchers have extended their evaluations of cross-sections to the sub-barrier region to address discrepancies between CC calculations and measured cross-sections of collisions between certain systems at very low energies. This effort revealed a steep falloff in

the cross-section of fusion at these energies, which was recognized as a hindrance in heavy-ion fusion at extremely deep sub-barrier energies [3, 16].

To clarify this point at this initial stage, Fig.1.1, which is taken from Ref.[1], presents a depiction of the features of enhanced fusion and hindered fusion for the system ^{64}Ni+^{64}Ni, serving as an example. The curves are coupled-channels CC calculations (red solid) and one-dimensional simple model calculations where couplings are ignored (black dashed). The fusion enhancement is indicated by the variation between the black curve and the experimental data, whereas the fusion hindrance at extremely low sub-barrier energies is demonstrated by the deviation among the experimental results and the red curve.

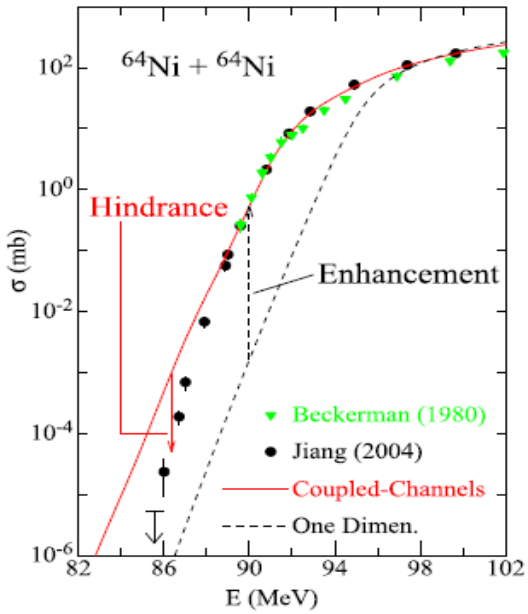

Fig.1.1 Fusion cross section for the system ^{64}Ni +^{64}Ni (data: Beckerman [4], Jiang [5]). Illustrating the impacts of hindered fusion and enhanced fusion.

The objective of this thesis is to examine the current state of fusion reactions involving heavy ions research specifically those occurring at energy levels significantly below the barrier, in particular focusing on the fusion hindrance phenomenon. Both experimental and theoretical investigations related to this topic have been reviewed up to the present day. After gaining a comprehensive understanding of these studies, the thesis will concentrate on a contentious topic in the literature: the reason behind and the mechanism by which the Sudden and Adiabatic models, two distinct approaches utilized for analyzing fusion reactions

theoretically, generate nearly identical cross sections even though they use different potential structures (shallow and deep potential functions).

This ongoing debate will be meticulously examined and clarified through the application of the supersymmetric phase equivalent potential concept, as outlined in Ref. [6]

Within this context, in Chapter 2 the essential theoretical background is presented to prepare the reader with the requisite physical knowledge as a foundation in this field, involving in particular, the most significant theoretical models to be able to clarify the fusion hindrance observed at heavy-ion fusion reactions, as many scientists have been working in this field since the discovery of the hindrance phenomenon in 2002.Chapter 3 involves our discussion on deep and shallow supersymmetric partner potentials considering Sudden and Adiabatic treatment results. The final Chapter proposes concluding remarks and an overview of the comprehensiveness of the work presented in this thesis.

CHAPTER 2
THEORETICAL BACKGROUND

For the current theoretical comprehension of the theory of fusions constructed by heavy ions, which encompasses the hindrance phenomenon that occurs below the fusion barrier, it is necessary to establish a strong base in the relevant research area. This includes formulating a clear statement of the issue raised by the work presented in the thesis besides providing physically meaningful solutions, which is one of the main motivations behind this chapter.

During the last quarter century, numerous papers reviewing the broad subject of fusion reactions involving heavy ions have been brought out see the related references in [1]. Many of these studies, since 2002, have been focused on the heavy-ion fusion hindrance at energy levels significantly beneath the fusion barrier. For a recent review, the reader is referred to Refs [7, 8]. Meanwhile, some new measurements and analysis on the fusion hindrance of systems composed of medium and light masses were also published subsequently. However here, through the present thesis work, we will focus solely on the fusion reactions involving heavy systems.

Fig.2.1, taken from [7], illustrates a standard potential plot between two nuclei, represented as a function of the distance r separating them. This plot involves two distinct interactions: firstly, the Coulomb interaction arises due to the positive charge of the nucleus, resulting in the long-range and repulsive force acting between the two nuclei. Secondly, when the nuclei are at a smaller distance, a short-range nuclear interaction, which is attractive and referred to as a strong interaction comes into play. At just the outside of atomic nuclei, namely beyond their surfaces, strong nuclear force almost dies away. Because of the cancellation of nuclear and Coulomb forces, the Coulomb barrier, typically arises at a distance R_b, larger than the touching radius R_{touch} where the two nuclei come into contact during a fusion reaction:

$R_{0-16} + R_{Sm-144} = r_0 A^{1/3} = r_0 \left[\left(16^{1/3}\right) + \left(144^{1/3}\right) \right] fm$, in which r_0 is taken as 1.2 *fm* or 1.4 *fm* depending on the nucleon density consideration as charge or matter distribution.

The energy range of the reaction system is established by the height of the Coulomb barrier, denoted by V_b, as $V_b = k\frac{q_1 q_2}{r} = \left(\frac{1}{4\pi\varepsilon_0}\right)\frac{(Ze)_{O-16}(Ze)_{Sm-144}}{R_b}$ *MeV*.

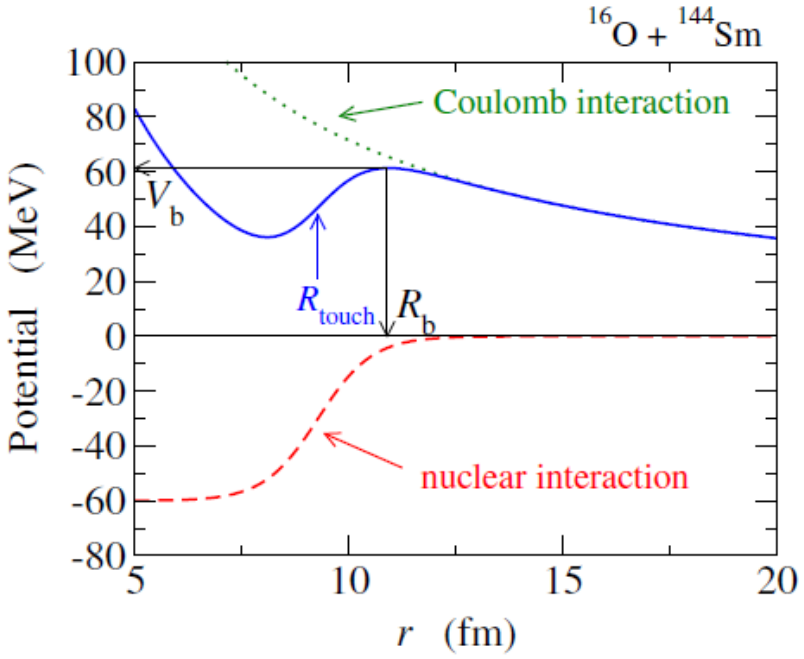

Fig.2.1 Description of the internucleus potential between two nuclei in relation to the distance separating them (the solid line). The $^{16}O+^{144}Sm$ reaction is commonly regarded as a standard instance. The Coulomb and the nuclear components are indicated by the dotted and the dashed lines, respectively. R_b and V_b indicate the Coulomb barrier's position and height, respectively. While Rt_{ouch} refers to the point at which the two nuclei touch each other.

In this thesis, an overview of sub-barrier fusion reactions occurring in the vicinity of the Coulomb barrier is presented in detail. The sub-barrier region is significant for the two clear reasons. One has to do with fusion processes that create super-heavy elements. Nuclear astrophysical reactions are the second obvious reason to talk about it, Fusion reactions that occur in stars, like the $^{12}C+^{12}C$ reaction, appear at exceedingly low energies, making the task of precise measurements of fusion cross-sections directly challenging. Therefore, fusion cross-sections measured at greater energies must be extrapolated to the energy range with reference to nuclear

astrophysics. To make dependable extrapolations, a profound comprehension of the way fusion behaves in the region below the energy barrier is of major significance.

In addition to the aforementioned reasons, sub-barrier fusion exhibits intriguing reaction dynamics in its own right. Firstly, the interaction between nuclear reaction and nuclear structure is of particular significance in a fusion that occurs below the energy barrier, as nuclear structure plays a crucial role in the process of nuclear fusion. In comparison to nuclear reactions that occur at high energies, this is different, they have much simpler reaction dynamics. Secondly, sub-barrier fusion reactions are an exemplary illustration of the many-particle tunnelling phenomenon. For fusion to occur, two nuclei must come close enough to reach the touching radius, and thus quantum tunnelling is the only means by which fusion can occur in the case where the incident energy is less than the Coulomb barrier as depicted in Fig. 2.1. It is worth noting that a variety of intrinsic degrees of freedom, such as collective vibrations and nuclear deformation with different multi-polarities in atomic nuclei, can influence quantum tunnelling.

Furthermore, fusion reactions of heavy ions offer an exceptional opportunity to investigate the energy dependence of the tunnelling rate by adjusting the incident energy, which is a marked difference from other tunnelling phenomena in nuclear physics like alpha decays, where the energy is predominantly determined by the decay Q-value. As such, heavy-ion fusion reactions can be regarded as an optimal platform to explore many-particle quantum tunnelling with numerous degrees of freedom.

Several review articles have already been released regarding sub-barrier fusion reactions. Although References [9, 10] delve into the theoretical parts of such reactions, Reference [11] provides a summary of experimental findings on sub-barrier fusion reactions based on the idea of distributions of fusion barriers. Meanwhile, References [1, 12, and 13] examine fusion reactions of heavy ions at energies significantly below the energy barrier, where fusion cross-sections seem to be hindered compared to the direct extrapolation of fusion cross-sections at sub-barrier energies.

2.1 Potential model and the Wong formula

The potential model, which takes into account structerless projectile and target nuclei without any excitation and supposes the existence of some potential between them, is the simplest method for studying fusion reactions. Assuming that the touching position has been reached, it is generally considered an appropriate estimation would be to state those fusion reactions automatically generate a compound nucleus, involving medium-to-heavy nuclei. Fusion cross sections $\sigma_{fus}(E)$ are then presented by [1, 7]

$$\sigma_{fus}(E) = \frac{\pi}{k^2}\sum_{\ell}(2\ell+1)P_{\ell}(E) \tag{2.1.1}$$

where E is the bombarding energy in the center of mass frame and $k = \sqrt{2\mu E/\hbar^2}$ is the wave number for the relative motion between the two nuclei with the reduced mass μ. In there ℓ is the orbital angular momentum for the relative motion, and $P_{\ell}(E)$ is the probability to reach the touching configuration [1, 7, 14, 15]. In the other words, $P_l(E)$ is the penetrability of the Coulomb barrier. An evaluation of this can be carried out, for instance, through the incorporation of a short-range absorbing potential, such as the Pauli repulsion that will be discussed in detail later, into an internuclear potential. Provided that it is suitably confined within the Coulomb barrier, this absorbing potential typically accounts for any process other than elastic scattering - such as fusion or transfer reactions - and approximately simulates the formation of a compound nucleus.

Wong has developed a simplified and concise formula [14], with an approximation of the Coulomb barrier as an inverted parabola, to incorporate the impact of quantum mechanical tunnelling through the barrier. This method has been employed [15] for measuring fusion cross-sections

$$V(r) = V_b - \frac{1}{2}\mu w^2 (r - R_b)^2 \tag{2.1.2}$$

For which the penetrability can be presented analytically as

$$P_{\ell=0}(E) = \frac{1}{1+\exp\left[\frac{2\pi}{\hbar w}(V_b - E)\right]} \tag{2.1.3}$$

Here, w is the frequency of the inverted harmonic potential while R_b is the barrier radius. For non-zero partial waves, Wong considered $\ell-$independent barrier position and curvature, and replaced P_ℓ with

$$P_l(E) = P_0(E - \frac{l(l+1)\hbar^2}{2\mu {R_b}^2}) \tag{2.1.4}$$

Finally, Wong replaced the sum in Eq. (2.1.1) by an integral [7, 14]

$$\sigma_{fus}(E) = \frac{\pi}{k^2}\sum_{\ell}(2\ell+1)P_\ell(E) \rightarrow \frac{\pi}{k^2}\int d\ell(2\ell+1)P_\ell(E) \tag{2.1.5}$$

To attain the so-called Wong formula presented by

$$\sigma_{fus}(E) = \frac{\hbar w}{2E}R_b^2 \ln\left[1+\exp\left(\frac{2\pi}{\hbar w}(E-V_b)\right)\right] \tag{2.1.6}$$

Despite potential approximations, the method outlined above is considered the fundamental approach for determining fusion cross sections as it relies on essential elements of physics. Coupled channels (CC) calculations, employing Schrödinger or similar equations, fall under this category and are utilized in subsequent sections.

However, similar to various other theoretical approaches, these calculations generate numerical outcomes rather than analytical formulas as seen in Eq. (2.1.6).

Fig.2.2, which is taken from Ref. [1], shows calculated fusion cross sections by (2.1.6) for the ^{16}O+^{154}Sm system. The figure indicates that the Wong formula is effective, aside from the area significantly beneath the Coulomb barrier where the formula outlined in (2.1.6) overestimates fusion cross sections for nuclei that considered being heavy. This is due to the parabolic approximation, as detailed in Eq. (2.1.2), employed in the Wong formula which predicts a narrower potential barrier than it actually is. Consequently, penetrabilities are overestimated, leading to a significant overestimation of fusion cross sections at energies considerably lower than the barrier.

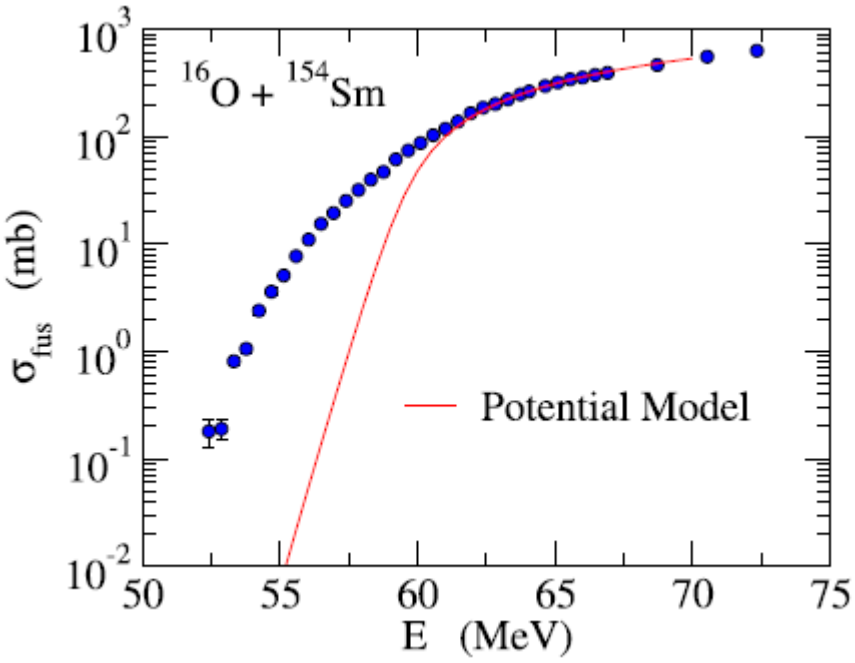

Fig.2.2 Potential model calculations for the $^{16}O+^{154}Sm$ system.

Once a potential is known, one should first estimate the appropriate fusion cross sections using a straightforward formula, such as the one proposed by Wong, Eq. (2.1.6). Despite the fact that, as was previously stated, although the potential model is not applicable to systems include heavy nuclei at energies lower than the Coulomb barrier, it still serves as a valuable reference point for discussing the effects related to the motion in fusion reactions of heavy ions. Various studies [1, 3, 5, 7, 8, 10, 12, 13, 15, 17-19] have established that heavy-ion fusion cross-sections are considerably enhanced at energies below the Coulomb barrier, due to couplings with nuclear intrinsic degrees of freedom, as in comparison to the predictions of Wong's simple potential model which is the subject of the following sections. Sub-barrier fusion reactions in heavy-ion systems, therefore, offer a useful illustration of environmental tunnelling phenomena.

2.2 Attempts to improve the potential model

According to the discussion above, there is a strong correlation exists between the low-lying collective configuration of the nuclei undergoing collision and sub-barrier fusion dynamics, thus in order to replicate the experimental findings, a more sophisticated calculation method like the coupled channels (CC) model is essential.

Recent developments attained in the scope of near and sub-barrier heavy-ion fusion reactions are evaluated here to analyze heavy-ion fusion reactions with the goal of providing a deeper physical analysis of these reactions than the straightforward potential model mentioned in the preceding section. This review will mainly focus on the hindrance phenomenon that occurs well below the barrier, with particular assurance on the analytical findings of the past decade.

Actually, initial studies on sub-barrier fusion demonstrated that cross-sections are heavily influenced by the low-energy collective modes of the nuclei involved in the collision, and probably by couplings to transfer channels as well. The coupled channels (CC) model, as discussed in Reference [2], has been highly effective in elucidating the experimental results.

For the physical and computational details of CC calculations the reader is referred to [12] whereas its short description is discussed in Appendix B. The signature of the related coupled channels calculations can frequently be earned from fusion barrier distributions. Standard CC calculations overestimate the cross-sections at deep sub-barrier energies because the slope of the excitation function, or the associated reaction cross-section, in a semi-logarithmic plot, keeps rising. This phenomenon was called a hindrance, and experts disagree as to where it came from physically. This is the primary driving force behind our thesis work. Recent theoretical advancements have also raised the possibility that this effect may be, at least in part, due to the Pauli Exclusion Principle, which will also be discussed in more detail in Sec (2.3).

The Argonne National Laboratory experiment [3, 16] that led to the discovery of the hindrance phenomenon revealed that the fusion cross-sections of ^{60}Ni + ^{89}Y display an unexpected trend far below the barrier, characterized by a rapid falloff that exceeds the predictions of conventional coupled channels (CC) computations. This created a new area for investigation and was quickly accepted as having a general impact, although one with varied effects whose origin is still under discussion and investigation in the community.

Several review papers have been released throughout the years, addressing different aspects of heavy-ion fusion and discussing recent discoveries and advancements. References [10] and [12] provide relevant reviews, the first one presenting an in-

depth theoretical analysis of many-body quantum tunnelling and the latter covering all aspects of heavy-ion fusion. Additionally, Ref. [17] offers a captivating review devoted to hindrance in heavy-ion fusion reactions.

2.2.1 Channel coupling effect with a repulsive nucleon-nucleon force

The coupled-channels formalism is now widely recognized as the appropriate language for analysing fusion reactions that occur below the Coulomb barrier. A significant piece of coupled channel calculations, see Appendix B, together with their outstanding results with a repulsive nucleon-nucleon potential [17-19] are summarized here. Since the appearance of [16] in the related literature at 2002, the hindrance phenomenon on heavy-ion fusion at energies significantly lower than the Coulomb barrier has been extensively explored through experimental and theoretical means.

According to Mişicu and his co-workers [17–19], the incompressibility of nuclear matter results in a thicker Coulomb barrier, which hinders fusion for reactions at extremely low energies. They also demonstrated how the consideration of a repulsive short-ranged nucleon-nucleon potential could lead in such an effective calculation to examine the hindrance problem of heavy-ion cross sections. Their calculations showed that, unlike a straightforward single-channel treatment, the standard usual CC model, which deals with the coupling of possible channel interactions such as vibrations, nucleon transfer, and excitation of low-lying states, is inadequate alone to explain and analyse the unexpected behaviour of excitation function seen through heavy nuclei. By taking into account Pauli repulsion in between fermions through the inner side of the fusion region, the researchers in [17-19] proposed to use a shallow potential for the entire-ion-ion interaction, instead of typically employed deep potentials, to remove this drawback in coupled channel calculations. This indicates that the representation of the interaction between nucleon quarks when they are so near to one another must include the required short-range repulsive potentials. One must first take into consideration the relevant earlier research in Refs [18, 19], which are the spirit of [17], in order to understand these approaches and imaginatively picture the findings.

The abrupt falloff in cross-sections, as mentioned earlier, cannot be accounted for by the conventional straightforward theoretical method of handling capture reactions, which involves quantum tunnelling through the relative barrier of the di-nuclear

system in coupling with various low-lying collective modes. Furthermore, at energies below a certain threshold, the coupled channels (CC) method fails to adequately describe the fusion process dynamics. The origin of this phenomenon is crucial to understanding the reaction process and may have significant repercussions for nuclear events that take place in stars. It might imply that below a specific energy threshold, the synthesis of heavy elements is hindered.

Mişicu and Esbensen [18] introduced a new mechanism in 2006 to account for the unexpected sharp decrease in fusion cross-sections at energies well below the Coulomb barrier. According to their proposal, the characteristics of nuclear matter when it reaches saturation hinder the significant overlap of the colliding nuclei, resulting in a sensitive shift in the nuclear potential inside the barrier. To confirm their hypothesis, the authors of [18] used a double-folding potential that includes a short-range Michigan-3-Yukawa (M3Y)-Reid effective nucleon-nucleon force with a repulsive core that simulates the nuclear incompressibility for complete overlap. In their letter, they reported that this potential, with an additional term, provides a satisfactory match to the coupled-channels calculations for the ^{64}Ni + ^{64}Ni fusion reaction. This additional term yields a shallow fusion potential with a nuclear, Coulomb, and angular momentum barrier, making it possible to perform a reliable analysis of the fusion reaction under consideration. For further information, the reader is referred to Appendix A.

To determine the features of the short-range repulsive core, it should be noted that an area of doubled nucleon density arises as a result of the fusion between the target and projectile once the distance R between the interacting nuclei becomes less than R_P and R_T, which represent the nuclear radii along the collision axis. The density doubling leads to a rise in the energy of the nucleons located in the overlapping region as discussed in Appendix A.

To demonstrate the form of this potential for a relevant scenario, Mişicu and his co-worker [18] compared in Fig. 2.3 the spherical heavy-ion potential for the symmetric di-nuclear system ^{64}Ni+^{64}Ni to deep potentials having different structure previously utilized.The variations in thickness and depth of these three potential behaviours in Fig. 2.3 through the inner region, where the overlapping occurs, are clearly seen. The usage of the M3Y+repulsive-Reid potential in combination with the appropriate folding potential function, which results in a shallow nature of the entire interaction potential term, is what causes this difference. Potentials like the Winther-Akyüz can offer reliable barriers, as shown in the figure below, but their inability to reproduce data well below the barrier suggests that the ion-ion potential has a different form in the inner part of the barrier, such as the M3Y+repulsive potential.

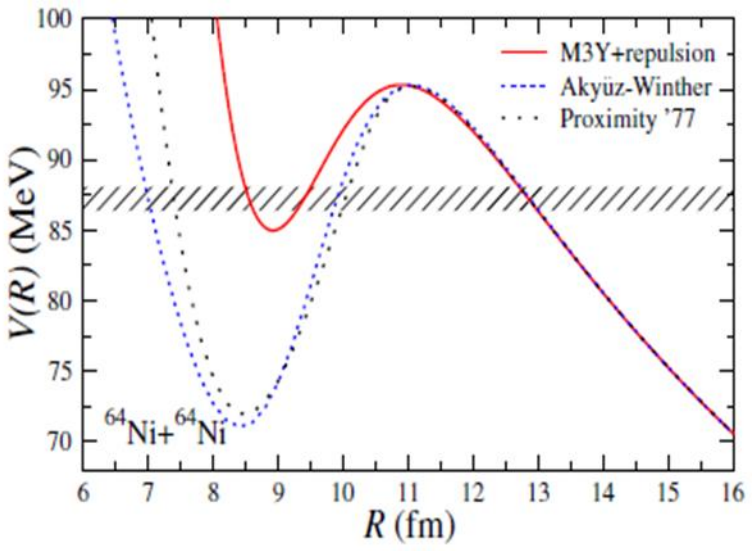

Fig.2.3 Different spherical ion-ion potentials for ^{64}Ni + ^{64}Ni.

With this consideration and from Fig.2.4, it is obvious that the CC model with M3Y+Repulsive short-range nucleon-nucleon potential (red curve), which agrees with the observed data throughout the whole domain of center of mass energies under investigation, provides the best analysis of the related fusion reaction. Winther-Akyüz potential and the other simple CC theoretical calculation without including coupling (NOC), such as couplings to the low-lying 2^+ and 3^- states, mutual excitations, and two-phonon quadrupole excitations, have no capability to reproduce the corresponding cross section data for the overall domain. Nevertheless,

CC calculations with Winther-Akyüz potential reproduce data well far below the Coulomb barrier, when compared to NOC calculation.

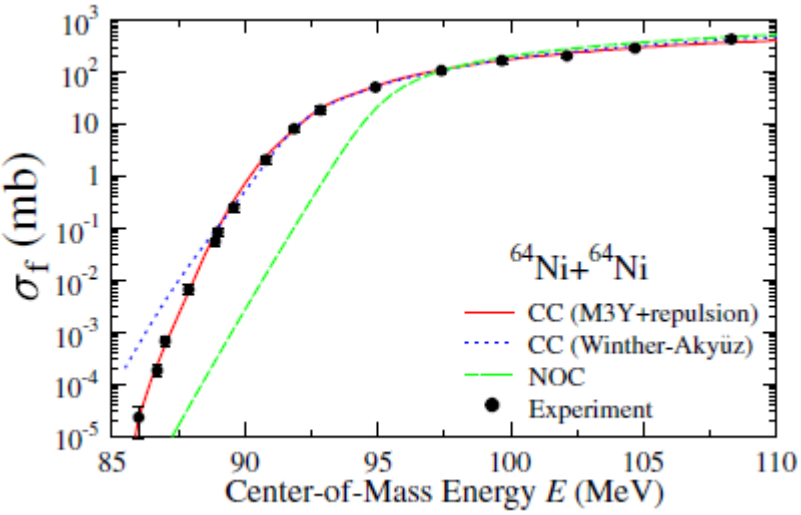

Fig.2.4 Different calculations in comparison to the experimental fusion excitation function for the ^{64}Ni + ^{64}Ni system.

Thus, the researchers from [18] noted that the exponential drop in the tunnelling probability is linked to the elimination of the region that is classically allowed at energy levels below a certain threshold after a series of straightforward but clear arguments. We are in fact faced with the presence of a small potential pocket inside the barrier as a result of this situation. They reached the conclusion that the experimental data can only be interpreted by introducing an amended form of the potential inside the barrier, at least for the case ^{64}Ni + ^{64}Ni. Many researchers in the same field have been impacted by this important issue, which will be covered in more detail in the next sections.

The interpretation of experimental evidence has been successful by the refined CC model calculations, which proposed both a shallower pocket and a thicker barrier are necessary to account for the estimated cross sections. These characteristics are surely elucidated by the M3Y +repulsion heavy-ion potential.

2.2.2 Test of the shallow nature of the nuclear potential

After just one year from the appearance of [18] in the literature, Mişicu and Esbensen published another work in [19] which is the extension of their previous study in [18] to elucidate the sharp decline in the fusion cross section at extreme sub-barrier energies for the symmetric di-nuclear system ^{64}Ni+^{64}Ni to another symmetric system, ^{58}Ni+^{58}Ni, and the asymmetric system ^{64}Ni+^{100}Mo. The nuclear equation of state's impact on the internal part of the nuclear potential leads to a decrease in the area where overlapping configurations are allowed in classical terms. This reduction results in a decline in fusion cross sections at bombarding energies considerably lower than the barrier in this model.

The fusion cross sections, *S* factors, and logarithmic derivatives for the systems mentioned above were calculated and compared with the experimental data using the coupled-channels method, taking into account couplings to the low-lying 2^+ and 3^- states in both the target and projectile in addition to mutual and two-phonon excitations of these states. Even at the lowest energies, there was a good agreement observed with the data

To investigate the hindrance in sub-barrier fusion in different cases, the authors suggested the use of two representations, building upon the work in [3], in order to clarify the issue of interest. This consideration also serves us as a stringent test case of using shallow nuclear potential in such treatments. Within this frame, the first one is the astrophysical *S* factor,

$$S = E\sigma(E)\exp(2\pi\eta) \tag{2.2.1}$$

where E is the center of mass energy, $\eta = Z_p Z_t e^2 / (\hbar v_{rel})$ is the Sommerfield parameter, being with Z_p and Z_t are the nuclear charges of projectile and target nuclei respectively, and finally v_{rel} is the beam velocity. For the systems under consideration, the experimental *S* factor increases as the bombarding energy decreases and tends to exhibit a maximum. The *S* factor is an important quantity for investigating the area within the barrier during low-energy fusion processes involving heavy ions, and it also amplifies structures in the excitation/cross-section function at energies below the barrier. This point will be justified soon in this section.

A second representation used in [19], to clarify the hindrance in sub-barrier fusions, is the logarithmic derivative [3]

$$L(E)=\frac{d\left[\ln(\sigma E)\right]}{dE}=\frac{1}{E\sigma}\frac{d}{dE}(E\sigma) \tag{2.2.2}$$

Examining the derivative of the *S* factor offers an insight into the correlation between the two depictions of low-energy fusion data, namely the *S* factor and the logarithmic derivative. From Eqn. (2.2.1) and (2.2.2), one gets the following expression

$$\frac{dS}{dE}=S(E)\left[L(E)-\frac{\pi\eta}{E}\right] \tag{2.2.3}$$

A maximum in the *S* factor means that $dS/dE=0$. This condition is met when the logarithmic derivative is

$$L_{CS}(E)=\frac{\pi\eta}{E}=\frac{\pi Z_p Z_t}{E^{3/2}}\sqrt{\frac{m_n}{2}\frac{A_p A_t}{A_p+A_t}} \tag{2.2.4}$$

where A_p and A_t are the mass numbers of the reaction partners and m_n is the nucleon mass. More physically, Eq. (2.2.4) is just the logarithmic derivative for a constant *S* factor.From [3]; it is well known that the logarithmic derivative $L(E)$ obtained from the experimental data intersects the curve $L_{CS}(E)$ exactly at the energy where the experimental *S* factor reveals a maximum. Denoting the energy and logarithmic derivative where this intersection occurs by E_S and $L_S=L(E_s)$ respectively. These two quantities are then related by the equation

$$L_S(E_S)=\frac{\pi Z_p Z_t}{E_S^{3/2}}\sqrt{\frac{m_n}{2}\frac{A_p A_t}{A_p+A_t}} \tag{2.2.5}$$

The *S* factor and the values of E_s and L_s where the logarithmic derivative obtained from measurements crosses with the logarithmic derivative for a constant *S* factor are not essentially unique or significant. They are simply a means of characterizing the unexpected rapid decrease in measured fusion cross sections, serving as a suitable substitute.

When the *S* factor makes it to its peak, the logarithmic derivative will have exceeded the expectations based on standard coupled-channels calculations. The benefit of using the *S* factor is that it provides a straightforward and direct measure of the fusion cross-section, whereas the logarithmic derivative, as described in Eq. (2.2.2), is derived more indirectly. Additionally, the energy E_0, as defined in the pioneering article [16], is model-dependent, whereas E_s and L_s are obtained without requiring any free parameters. Taking into account the comprehensive discussion in Refs [1] and [3], one arrives at

$$E_S = 0.495\left[Z_p Z_t \sqrt{\frac{M_p M_t}{M_p + M_t}} \right]^{2/3} MeV \tag{2.2.6}$$

Where E_S and L_S are given in units of MeV and $1/MeV$, together with Z_p and Z_t being the respective charge numbers and M_p, M_t are the respective nuclear masses of projectile and target nuclei in units of nucleon masses. In sum, by integrating the two representations, the logarithmic derivative and the *S* factor, in [3], the researchers managed to formulate a straightforward physical empirical equation that describes the energy at which the *S* factor attains its highest point for reactions involving rigid partners.

Additionally, based on the previous considerations, it is anticipated that to account for the Pauli Principle, the interaction potential of two colliding nuclei includes a repulsive core, which forbids the overlap of wave functions between two fermionic systems, as illustrated in Fig.2.5. The specific shape and strength of the repulsive core depend heavily on whether the collision is adiabatic or sudden, which will be discussed in detail through Chapter 3.

From the Fig.2.5 below, which is taken from [19], it is obvious that the addition of short range repulsive nucleon-nucleon force, to the usual nuclear folding potential, together with the Coulomb potential and angular momentum barrier $\left(= L(L+1)\hbar^2 / 2\mu r^2\right)$, describing the interaction between two heavy nuclei, has a different shallow structure when compared to the others. This shallow structure, representing Pauli repulsion, in general leads to physically acceptable analysis of fusion reactions with heavy-ions, unlike A-W and M3Y potentials. Because of their

lower barriers and abrupt decreases in the inner region, the M3Y and A-W potentials cannot accurately reproduce the data.

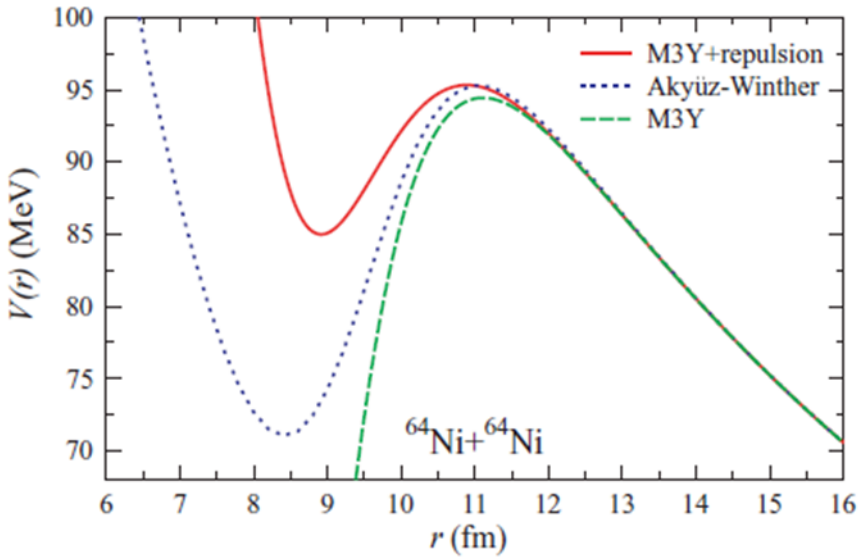

Fig.2.5 Observation of the double-folding nuclear potentials (with and without the presence of repulsion) and the Akyüz-Winter potential for the system ^{64}Ni+^{64}Ni.

The Fig 2.6 of Ref. [19] displays the Coulomb plus nuclear potential profiles for four heavy-ion systems. The authors present solid curves based on their M3Y+repulsion potentials, and short-dashed curves based on the A-W potential. Their analysis reveals that the predicted pockets for M3Y+repulsion potentials are notably shallower than those estimated by the A-W potential. Additionally, the dashed region in each panel of the figure highlights the energy E_s, at which the experimental S factor attains its maximum.

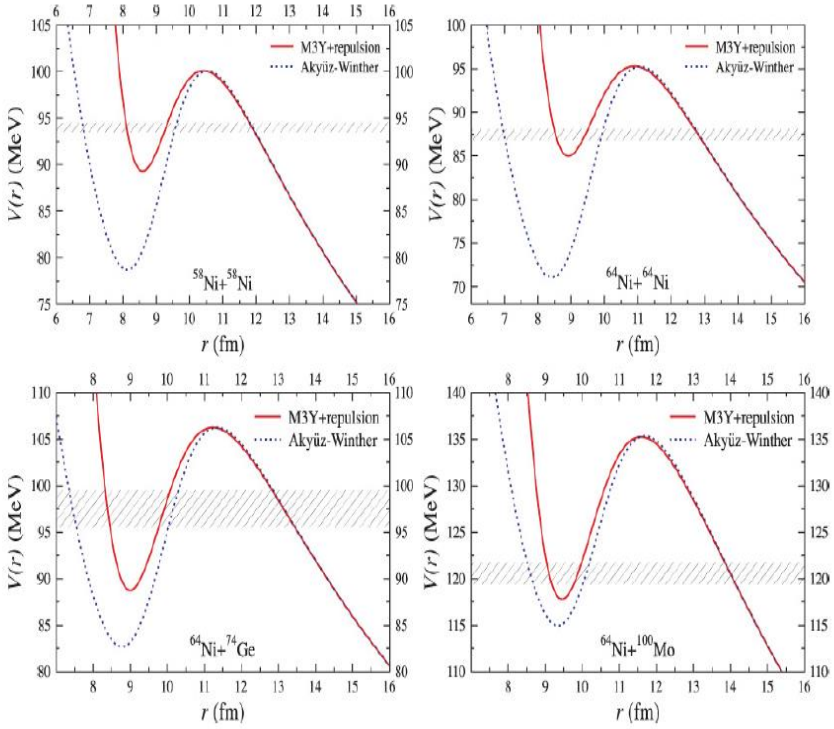

Fig.2.6 Ion-ion potentials for various systems

The effect of shallow potential in coupled channel calculations of [19] is also illustrated below, Fig.2.7, through the cross section analysis (with and without coupling), in which it is clearly seen that the nuclear potential with a repulsive piece (M3Y+repulsive) is the best description of the observables in such reactions.

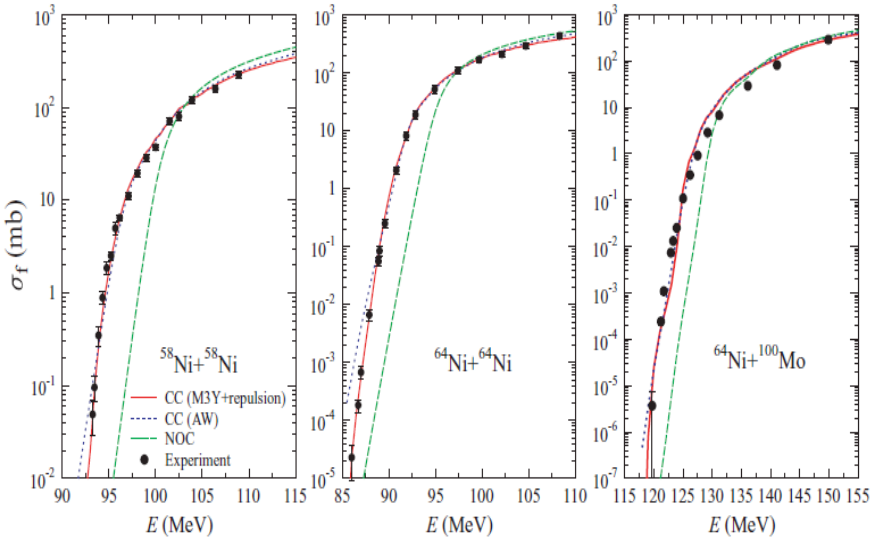

Fig.2.7 Comparison different treatments of fusion excitation functions for various systems.

In Fig.2.8, the researchers in [19] also compared the experimental *S* factors for different systems with those determined with the M3Y+repulsion and the A-W potentials. The shallow nature of the repulsion model well describes the data that is available and, more significantly, recreates the experimental *S* factor's tendency to yield a maximum. However, for the other treatments, there is already a clear discrepancy with the data. The calculations performed with M3Y plus repulsive piece also predicts maxima at lower energies.

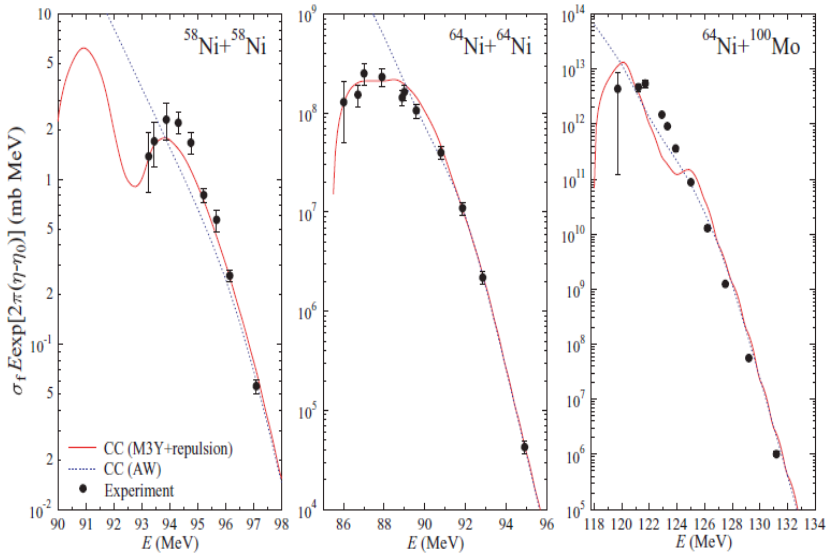

Fig.2.8 The experimental *S* factors for the different systems in comparison with CC calculations carried out using the M3Y+repulsion and A-W potentials.

Fig.2.9, quoted from [19], shows a graph of the logarithmic derivative for the energy-weighted cross-section in several heavy-ion interactions. This figure provides that the usage of the (M3Y+repulsion) potential provides a lucid depiction of the available experimental data. As anticipated from the response of the *S* factor, *L (E)* exhibits a peak just above the constant S-factor limit.

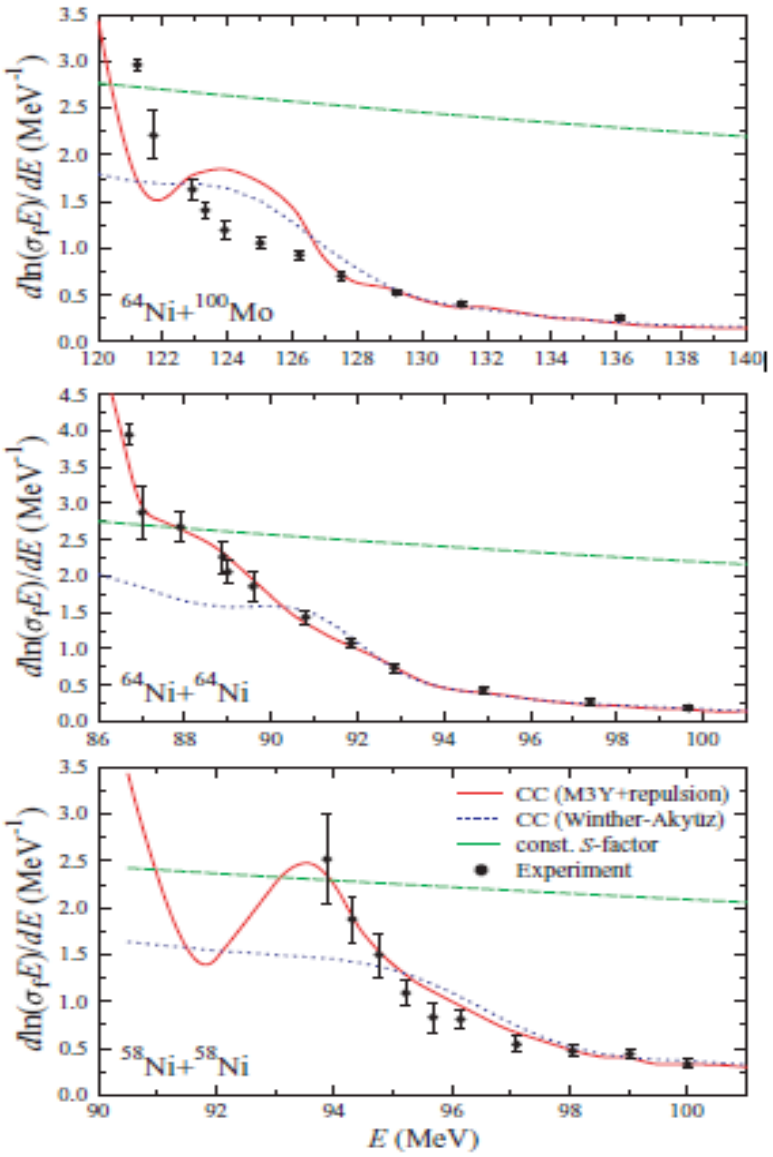

Fig.2.9 Logarithmic derivatives of the energy weighted cross sections for several heavy-ion interactions

Overall, for the various fusion reactions studied in Ref. [19], the authors observed a substantial association between the minimum of the potential pocket V_{min} and the determined reference energy E_S, obtained through the experiments, where the S factor attains its maximum value. A comprehensive investigation of fusion reactions across a broader range of $Z_p Z_t \sqrt{\mu}$ parameter values has established this evident relationship and supported the concept of a repulsive core when dealing with overlapping configurations, which will be argued through the present thesis work.

2.2.3 Concluding remarks on these amendments

Until about two decades ago, the analysis of low-energy fusion reactions involved a basic model discussed in Sec.2.1. This model utilized a local, one-dimensional real potential barrier that was created by attractive nuclear and repulsive Coulomb interactions. The assumption made was that absorption into the fusion channel takes place within the barrier region following quantum tunnelling. The potential's shape, location, and height were described using a small number of parameters that were adjusted to match the observed cross-sections.

The sub-barrier fusion cross sections for interactions of heavy nuclei are substantially bigger than those predicted from such a simple description, according to several of experiments carried out in the early 1980s see, for example, [4] and also Fig.2.2. The deficiency of the one-dimensional model for sub-barrier fusion was demonstrated precisely by obtaining the effective one-dimensional fusion barrier through the inversion of experimental data [9, and the references cited therein].

Along this line, in the previous subsections (Sec.2.2.1 and Sec.2.2.2) we discussed the adjustments to the simple model treatment made by CC calculations as a result of Mişicu and his collaborator's theoretical contributions. In there the authors accounted for the low-energy phenomenon arising from the presence of extra repulsion resulting from incompressibility and Pauli repulsion between fermions of target and projectile nuclei in the nuclear interaction of two vigorously overlapping nuclei. In these works a specific category of sub-barrier fusion reactions consisting of different projectile and target mixtures has been nicely proposed.

The theoretical contributions of Mişicu and his collaborator Refs [18, 19] led to the emergence of CC calculations.These investigations, which were performed for such reactions at extremely low energy, made it evident that the primary reasons for the hindrance to fusion are a thicker Coulomb barrier and a shallow nuclear potential behavior. From Figs (2.8) and (2.9) above, the computation of the astrophysical *S* factor and logarithmic derivative *L (E)* with respect to incident projectile energies, which are well discussed above, provided an explanation for the accuracy of such calculations. Additionally, it has been confirmed once more that the astrophysical *S* factor maximum that appears when energy approaches the lowest observed cross-sections is real.

By taking into account a proper nucleon-nucleon potential, this systematic deviation from the anticipated performance prescribed by the straightforward coupled channel calculations with Woods-Saxon (WS) potentials was eliminated, changing the full nuclear potential inside the overlapped region of heavy ion fusion interactions. Unlike to typically standard coupled channel calculations, this consideration results in a shallow depth for the nuclear potential, giving CC calculations the capability to accurately describe and analyse such reactions at extreme sub-barrier energies. Additionally, the examination of the logarithmic derivative *L (E)* from the study above makes it especially evident that previous calculations using standard CC calculations were unable to replicate the low-energy data points from the measured fusion cross-sections. From Fig.2.9, for energies that fall beneath a particular threshold (E_S), Eq. (2.2.6), as energy decreases, the experimental values of *L(E)* exhibit a sharp rise, in contrast, the theoretical values indicate a considerably lesser increase, excluding some specific oscillations..

For a comprehensive review of [18,19], together with an extension of these calculations involving analysis of many different fusion interactions and also significant details of nucleus-nucleus plus a proper choice of repulsive nucleon-nucleon interaction potentials, the reader is referred to [17].

2.3 Discussion on Pauli repulsion

As the projectile and target nuclei approach each other, the density overlap leads to increase in the prominence of Pauli blocking effects. This leads to the existence of a non-negligible Pauli repulsive interaction as well as the attractive nuclear interaction and repulsive Coulomb interaction amidst the collision of the two nuclei. Recently, Simenel and colleagues [21] proposed that the Pauli Exclusion Principle causes an increase in short-range repulsion in the ion-ion potential. They employed the density-constrained frozen Hartree-Fock method to precisely calculate the bare potential, including the Pauli repulsion. Similar to the phenomenological approach of the M3Y+repulsion interaction, a shallow pocket is presented in the resultant potential, which reduces the probability of tunnelling, leading to a relatively accurate reproduction of low-energy experimental data. Their microscopic calculations do not anticipate any repulsive consequences resulting from the incompressibility of nuclear matter, which is then assumed to simulate the impact of Pauli repulsion. This suggests a possible connection between fusion hindrance and Pauli blocking.

Overall, this finding suggests that the Pauli blocking effect prevents the synthesis of compound nuclei in regions of strong density overlap between projectiles and targets at very low collision energies. In actuality, the long-standing issue of deep sub-barrier fusion hindrance can be resolved by considering the contribution of Pauli repulsion. Therefore, the research presented in [21] aims to investigate the impact of the Pauli Exclusion Principle on the tunneling of sophisticated systems in the context of nuclear physics, which displays an excellent platform for testing concepts related to the quantum many-body problem.

At close distances, the Pauli Exclusion Principle creates a repulsive force between composite systems consisting of identical fermions, like the hard-core repulsion between two nucleons, which results from the presence of identical quarks of the same color in both nucleons. Therefore, the nucleus-nucleus potentials utilized to simulate reactions such as the fusion under consideration should incorporate the Pauli repulsion.

Reference [25] suggested that it would be beneficial to have a theoretical approach to precisely compute the repulsive section of the ion-ion potential utilizing the Pauli Exclusion Principle. Simenel and colleagues [21] have followed this approach, as

they calculate the bare nucleus-nucleus potential using the density-constrained frozen Hartree-Fock method, which exhibits a repulsive core inside the Coulomb barrier owing to Pauli blocking. This indicates that the fusion hindrance phenomenon is partly attributable to this effect.

As a result, researchers have introduced a Pauli blocking potential [26-28], arising from antisymmetrization, to substitute the exchange term in the conventional Michigan-3-Yukawa (M3Y) nucleus-nucleus potential, as outlined below:

$$V_N(R) = \int dr_1 dr_2\, \rho_p(r_1)\, \rho_t(r_2)\, g(s) + V_P(R) \tag{2.2.7}$$

with

$$g(s) = c_1 \frac{\exp(-4s)}{4s} - c_2 \frac{\exp(-2.5s)}{2.5s} \tag{2.2.8}$$

In Eq. (2.2.7), R denotes the distance between the center of mass of the two colliding nuclei and $s(= R - r_1 + r_2)$ is the distance between a nucleon in the target and a nucleon in the projectile. The Pauli blocking potential $V_P(R)$ in (2.2.7) can be derived by

$$V_P(R) = \int \rho_p(r) V_P^s(R + r)\, dr \tag{2.2.9}$$

The parameters and in Eq. (2.2.8) are the properly chosen strengths of the Yukawa interactions. For convenience, this nuclear interaction in (2.2.7) is labelled as M3Y + Pauli potential. The density distribution of the nuclei adopted in Eq. (2.2.7) is given by the standard Fermi form,

$$\rho_i(r) = \frac{\rho_{0i}}{1 + \exp(r - R_{0i}/a)} \tag{2.2.10}$$

where R_{0i} and a are the half-density radius and diffuseness parameters for the projectile $(i = p)$ or target $(i = t)$.

The calculation utilizes the double-folding integral of the proton-proton Coulomb interaction to determine the Coulomb potential.

$$V_C(R) = \int dr_1 dr_2 \frac{e^2}{s} \rho_{pp}(r_1) \rho_{pt}(r_2) \tag{2.2.11}$$

where ρ_{pp} and ρ_{pt} denote the proton density distributions of the projectile and target nucleus, respectively.

In the light of all these discussions above, together with Ref. [26] and also the related references therein, one can define $V_P(R)$ as

$$V_P(\rho_i) = 4515.9\rho_i - 100935\rho_i^2 + 1202538\rho_i^3 \tag{2.2.12}$$

Obviously, the nuclear potential used in these calculations is derived from the standard Michigan-3-Yukawa-Reid effective nucleon-nucleon interaction and the M3Y + Pauli potential, in which the Pauli blocking potential is used to replace the exchange term from the antisymmetrization condition, as is covered in more detail in the frame of reference of [26]. As an example, the corresponding result for $\alpha + {}^{208}Pb$ system is shown below, which is taken from Ref. [26].

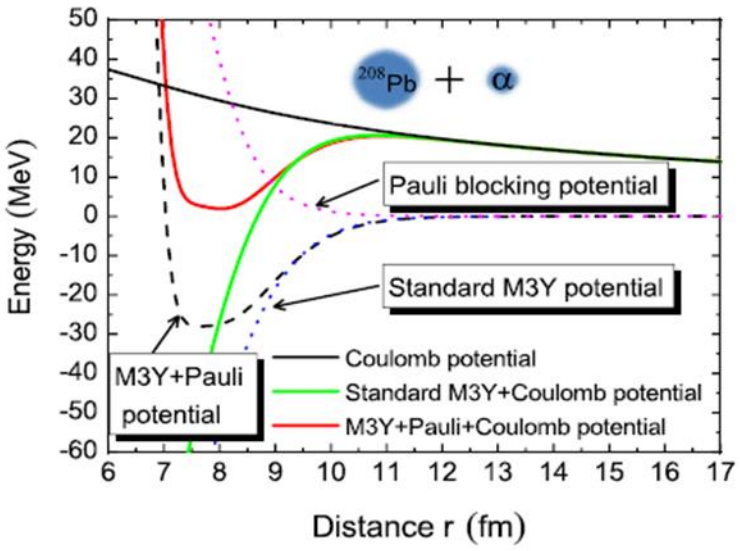

Fig.2.10 Assessment of the overall potential produced from the M3Y + Pauli potential (red solid line) with the one gained from the standard M3Y potential (green solid line) for the system α + ^{208}Pb. The Coulomb potential involved is the double-folding potential (black solid line). The Pauli blocking potential, standard M3Y potential, and M3Y + Pauli potential are illustrated by the pink dot line, blue dot line, and black dash line, respectively.

In [26], the authors compared the total potential for $\alpha + {}^{208}Pb$ system gained from the M3Y + Pauli potential to the standard M3Y-nuclear potential. The variables of the density distribution of the target nuclei used in the calculations can be found in [26]. The Coulomb potential dominates the behavior of both potentials in the region that is external. However, the significance of the Pauli blocking effect increases as the colliding nuclei get closer and their density overlaps. Consequently, the total potential resulting from the M3Y + Pauli potential has a shallow pocket in the inner region, in contrast to the potential acquired from the standard M3Y potential. This shallow pocket is similar to the one that appeared in the sudden model when taking into account the incompressibility of nuclear matter [17-19].

CHAPTER 3
DEEP SUB-BARRIER HINDRANCE

For fusion reactions constructed by heavy ions discussed in the earlier sections, experimental results have demonstrated that the fusion cross-sections decrease considerably more rapidly at energies below the Coulomb barrier compared to the predictions originating from theoretical extrapolation of fusion cross-sections obtained from coupled channel calculations. At this stage, we are now aware that the two-body potential description barely, without consideration of excitations for interacting nuclei, may fail. Subsequently, in reference [29], it was suggested that for the sake of replicating the cross-sections of these fusion reactions, a shallow potential is required. Two theoretical models have been proposed to explain the fusion hindrance at extremely low sub-barrier energies, one based on the sudden approximation by Mişicu and Esbensen [18, 19], and the other based on the adiabatic approximation by Ichikawa et al. [23, 24].

Fig.3.1 depicts a schematic representation of the contrast between the sudden and adiabatic models. As was clearly covered in the previous section, one often takes into account a shallow and thick potential barrier in the sudden model, as presented by Dasso and Pollarolo [29]. Referring to Eq. (A.2) and Fig.A.1 in Appendix A, a repulsive core is added to a double folding potential in Ref. [18, 19], where the repulsive section is built using the same procedure as the double folding but with a repulsive zero-range interaction. The crucial assumption underlying this model is that the reaction occurs at such a high fast that the density in the region where the projectile and target nuclei overlap doubles. This implies that the increase in potential energy at the origin caused by the repulsive core is equal to the energy increment of nuclear matter from its normal density to twice that density. Therefore, the outer region of the potential is sourced from the double folding model, while the inner region takes into account the phenomenological repulsive core, which represents Pauli distortion induced by the saturation property of nuclear matter. It has been shown that this shallow potential accurately replicates the rapid fall-off

phenomenon observed in heavy ion interactions discussed in previous sections using CC calculations.

It should be noted that the source of the repulsion in the region of overlap between the two nuclei attributed to the Pauli Exclusion Principle, as highlighted in Refs. [21, 26, 28], which extensively discussed in Section (2.3).

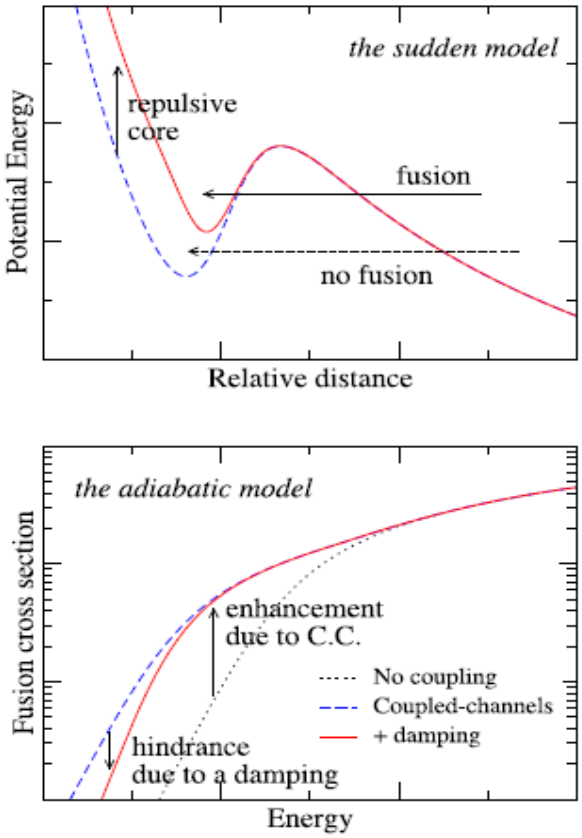

Fig.3.1 The illustration taken from [1] shows a schematic comparison of the sudden model with the adiabatic model for the hindrance of deep-sub barrier fusion.

Calculation results based on the sudden model have already been discussedand shown in Sections (2.2.1) and (2.2.2).

In the adiabatic model, it is assumed that the internuclear potentialeffortlessly connects to a potential of a single nucleus, which is frequently characterized by the liquid drop model, as opposed to the sudden model. This potential is referred to as the adiabatic potential after contact, as it minimizes energy at every internuclear

distance. Additional information on the potential structure in the adiabatic model can be found in Appendix C.

Continuing the coupled-channels calculations in spite of the nuclei touching each other can lead to double-counting the effect of excitation, as the adiabatic potential has already accounted for the primary effect of excitations [10]. The adiabatic model, after the touching point, significantly reduces the coupling effect [23, 24]. Thus fusion hindrance in the adiabatic model is a result of channel-coupling effects being quenched, whereas in the sudden model, hindrance is attributed by a truncation of high partial waves caused by a shallow potential.

3.1 Theoretical models: sudden versus adiabatic

The impact of the linkage between nuclear structure and translational motion can be analysed using two extreme cases. The initial situation is the sudden limit, where the energy levels of the internal system decayed. The second situation is the adiabatic limit, where the internal system crosses the barrier to its ground state, and its first excited state has a very high energy level.

In order to derive analytical outcomes that provide a theoretical structure for understanding the process of fusion, adiabatic and sudden approximations are particularly helpful. The data are reasonably well described by sudden approximation for deformed nuclei when the excitation energies are quite low. The sudden approximation is applicable in diminishing the size of channel coupling in rotation-vibration coupling.

The sudden approximation leans toward overstating the tunnelling probability at energies considerably below the barrier if the internal system's excitation energy is large. In fact, Esbensen and his co-workers [22] showed that the sudden approximation places an upper bound for the tunnelling probability when the energy is below the barrier.

Unlike the sudden model, the adiabatic method considers the formation of a neck between the colliding nuclei, where the interaction progresses from a two-body to a one-body potential, as discussed in Appendix C. References [23] and [24] introduced a reduction in the coupling form factors in the overlap region at distances between the ions that are closer to the touching point. It was proposed that this might result

from the quantum vibrations of the projectile and target being damped close to the touching point. To put it another way, the term "damping factor" refers to the gradual shift from sudden to adiabatic processes, or from a two-body system to a unified di-nuclear system.

The adiabatic model, which employs the Yukawa-plus-exponential (YPE) potential, produces fusion cross sections, S factors, and logarithmic derivatives that closely match experimental results [24] for a variety of systems. The authors observed that the energy at the point of contact has a significant correlation with the threshold energy at which the hindrance phenomenon occurs, except for medium-light mass systems.

In order to differentiate between the sudden and adiabatic models, average angular momentum $\prec \ell \succ$ of the compound nuclei can be compared. In the two models at energies lower than the threshold where hindrance occurs, $\prec \ell \succ$-values are remarkably different, see Fig 3.2.

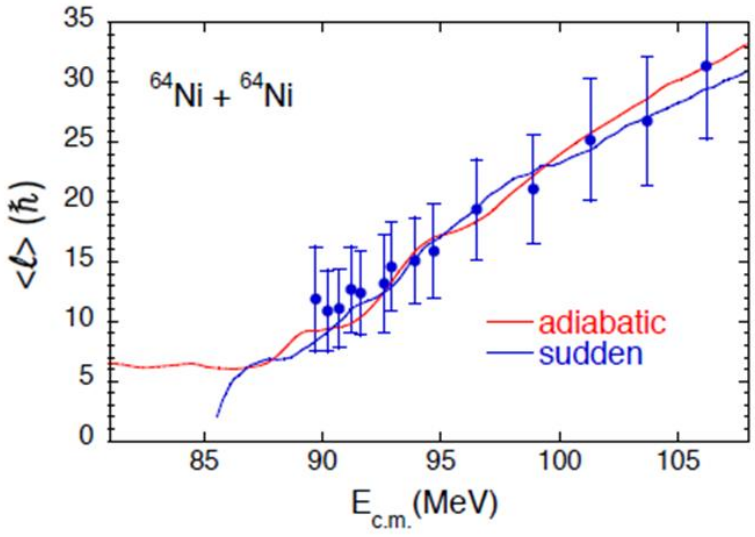

Fig.3.2 Relationship between incident energy and average angular momentum of the compound nucleus for ^{64}Ni + ^{64}Ni. Quoted from [13]. The M3Y+ repulsive potential was employed to generate the outcomes of the sudden model.

The mathematical form of this quantity will be discussed through Eq. (3.3.5) in Section(3.3) Estimated $\prec \ell \succ$ value within the frame of sudden model exhibits substantial suppression at low energies due to the cut-off of high angular-momentum components in partial waves caused by the shallow potential pocket. In contrast, the adiabatic model utilizes a damping factor that affects each partial wave cross-section, leading to higher angular momentum $\prec \ell \succ$ content for the compound nucleus less than the hindrance threshold. Therefore, it is crucial to determine the mean angular momentum at energies below the barrier.

Fig.3.3 presents the outcomes of the following examinations [24] conducted in the sudden and adiabatic models. As long as the excitation function is concerned, the outcomes of the two models are almost identical. Measuring at even lower energies will be necessary to discriminate between the two approaches because this is where the predicted S factor shows noticeable discrepancies, making measurements in this range particularly intriguing but also extremely difficult.

Despite the fact that the physics behind the hindrance varies in each, it should be emphasized that both the sudden and the adiabatic models highlight the significance of the dynamic phenomena occurring during the contact between two nuclei colliding.

Overall, it remains unclear which model - the adiabatic or sudden approach - explains the hindrance phenomenon better. The adiabatic approach accounts for the potential value at the point of contact and uses damping of coupling form factors at lower energies, whereas the sudden model employs a coupled-channels approach and a two-body potential, resulting in a shallow potential pocket. Without precise measurements, it will be challenging to differentiate between these two models.

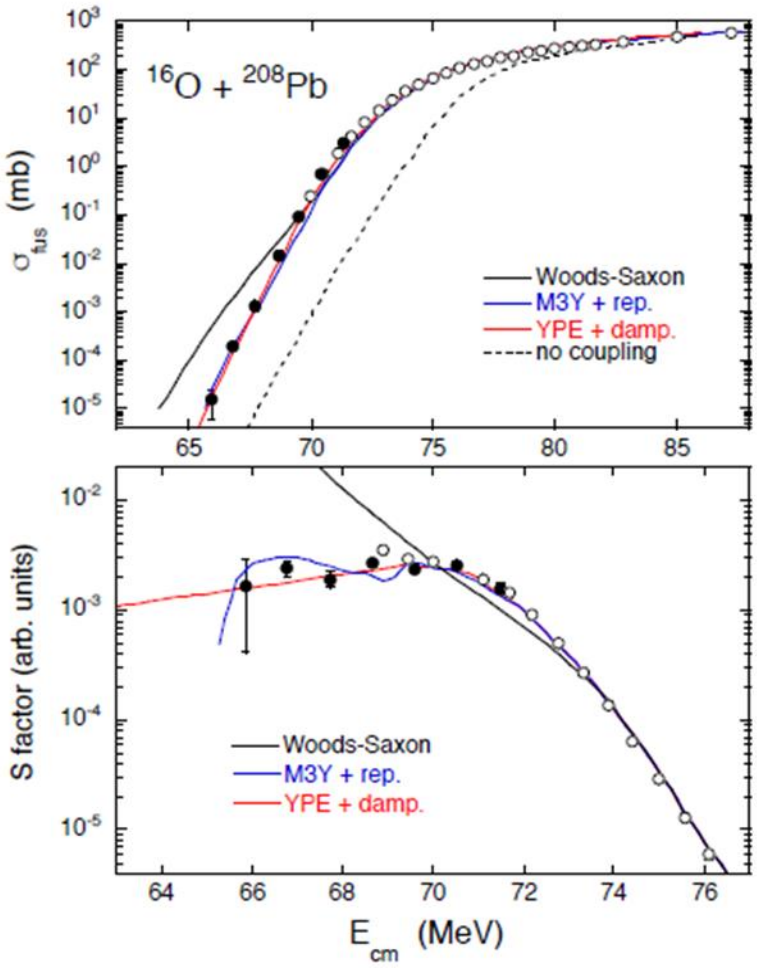

Fig.3.3 The upper panel shows the fusion excitation function, while the lower panel displays the astrophysical *S* factor of $^{16}O + ^{208}Pb$ compared to several CC calculations. Taken from [13].

3.2 A remark on deep and shallow potentials

In contrast to the adiabatic model which corresponds to deep potential, it seems that the sudden model is associated with a relatively shallow potential between the two nuclei during collision. Given the extensive discussion in [21], it is possible that the discussion of potential depth will be a little more complicated. In other words, a shallow (a deep) potential may not always be related to the sudden (the adiabatic) model. First of all, even though it is generally agreed upon that the Pauli principle results in a repulsive core, an alternative interpretation of the Pauli principle that involves Pauli attraction instead of repulsion remains a possibility. It should be noted that the main purpose of the Pauli principle is to reduce the amplitude of the radial wave function in proximity and that both the Pauli repulsion and the Pauli attraction can accomplish this objective in a comparable manner.

Fig.3.4 illustrates schematically the fusion dynamics with a shallow nucleus-nucleus potential (sudden model) and a deep inter-nucleus potential (adiabatic model).

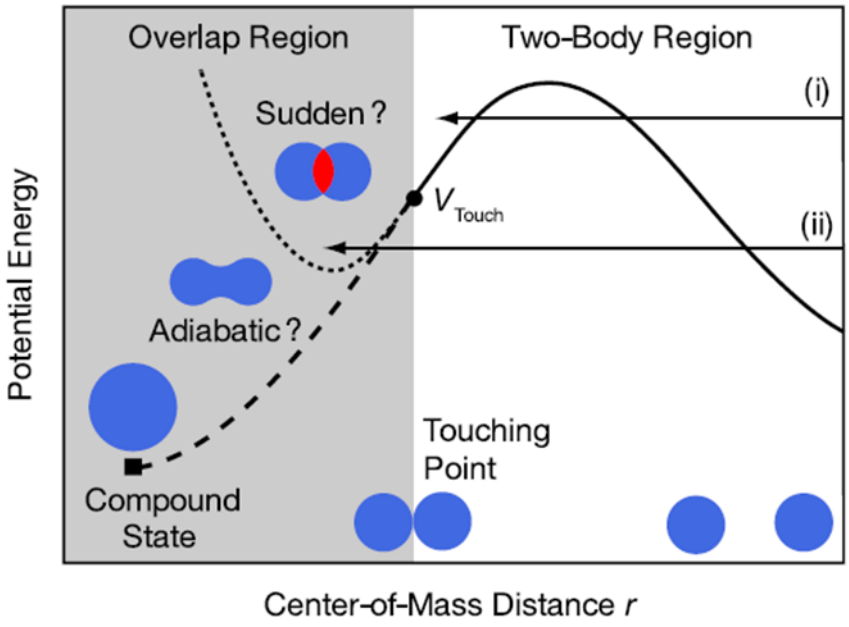

Fig.3.4 The internuclear potential and the fusion reaction dynamics examined in the sudden and adiabatic models. Taken from Ref. [24].

3.3 Supersymmetry between deep and shallow potentials used by sudden and adiabatic models

Employing a local potential is a desirable approach for characterizing the interaction in the middle of two combined particles, as it can effectively capture the bound states originated from the interacting particles and their scattering behaviour. However, due to the internal structure of these particles, there may be some confusion between two families of potential states: shallow potentials, which only have physical bound states, and deep potentials, which also have nonphysical bound states that simulate the Pauli principle's effect on the constituent fermions [31, 32].

Even though there are differences in their bound spectrum, potentials can be phase equivalent, meaning they have the same scattering matrix at all energies. Therefore, it is crucial to study the connections between phase equivalent potentials that vary in their bound spectrum, which is a significant physical concern.

Supersymmetric quantum mechanics [31] offers a potent mechanism for this investigation in the single-channel case because it permits the removal of bound states from a given deep potential without changing its phase shift.

In coupled-channel cases employed in the heavy-ion fusion interactions of interest in the present work, the distinction between deep and shallow potentials is doubtful. In nuclear physics, a crucial instance is the simultaneous presence of highly distinct families of nucleon-nucleon potentials: shallow potentials such as the one used by sudden models and deep potentials like the one used by adiabatic models utilize an extra non-physical bound state to simulate the underlying quark structure (refer to Fig.A.1)to resolve such uncertainties computation of phase-equivalent potentials was effectively expanded to coupled channels, using supersymmetric quantum mechanics as an optimal technique for this analysis [32].The authors of [32] demonstrated clearly that a shallow effective phase equivalent potential can be created by eliminating the deep non-physical bound state.

In qualitative agreement with other shallow potentials that already exist in the relevant literature, such shallow potentials produce a repulsive core. As stated in references [6] and [32], the deep potential wave functions have a node. In agreement with the singularity modification, this node vanishes from the shallow potential wave function and is substituted by an r^3 behavior close to the origin. The works in [6] and

[32] further demonstrated that both wave functions exhibit extremely similar asymptotic behaviour. The fact that this holds true for scattering states also supports the phase equivalence of the two potentials. In conclusion, just like it does in the single-channel situation, in the case of coupled channels, the use of supersymmetric quantum mechanics enables the formation of phase-equivalent potentials [32].

This short discussion reveals the hidden supersymmetric relation between the sudden and adiabatic model analysis of fusion observables for heavy ion interactions. Additionally, at this stage considering the work in [6] which investigates wave function-sensitive properties of the supersymmetric potentials by a halo transfer reaction, It is helpful to keep in mind that the shallow partner and the deep potential, employed in the fusion process to compute the entrance and exit channel wave functions, have similar phase shifts. As a result, any variation in physical properties, such as the related cross-section analyses, can be solely attributed to the wave functions of the partner potentials.

In order to clarify this matter, the researchers in [6] conducted through investigation of the properties of deep nuclear interactions. They accomplished this by explicitly constructing phase-equivalent potentials (PEP) that were free from the unphysical deeply bound states of the original potentials. The research demonstrated that to preserve the energy behaviour of the phase shifts, the central potentials needed to be repulsive and singular at short distances, with an additional shallow attractive component in the intermediate range. By reconstructing the potentials (PEP), the resulting relative motion wave functions were found to closely resemble those generated by deep potentials beyond the core region but lacked the radial node at short distances. Consequently, both types of potentials were expected to exhibit rather different off-shell behaviours and perhaps lead to qualitative differences in their outcomes. However, interestingly, no significant variation was observed in the *rms* radii calculated from these two very different two-body interactions. However, if the experiment necessitates a decrease in observables, it seems that a deep potential, which offers a short-range non-local contribution to the potential, may be required.

The authors in [6] employed phase-equivalent two-body potentials with varying numbers of bound states to investigate the ^{11}Be(p, d)^{10}Be transfer reaction and compared the results to the corresponding physical observables. By utilizing such

phase-equivalent two-body potentials in the three-body treatment of analysing the (p, d) reaction of interest they discovered [6] that the outcomes were almost indistinguishable. Therefore, their analysis indicated that the slight difference in wave function behaviour at short distances between deep and phase-equivalent shallow potentials, caused by an extra node within the core of the deep potential, is insignificant for the examination of these reactions, even though these potentials have matching behaviour at longer distances.

To summarize, the supersymmetric formulations employed in [6] primarily focused on addressing the Pauli Exclusion Principle in bound systems. This is achieved by assuming the presence of Pauli-forbidden states in the two-body potentials leading to the construction of corresponding phase-equivalent potentials without such states. The original deep potentials include unphysical terms that correspond to identical fermions being in the same states at short distances. These terms are removed, which forces the particles to occupy higher orbits, resulting in the requisite repulsion to avoid violating the Pauli principle

Therefore, in the light of the research results of [32] and [6] discussed above, we concluded that although the structures of the potential functions employed in these analytical treatment procedures are very different from one another, there should be a strict relationship between the potentials used by sudden and adiabatic models, as in supersymmetric phase equivalent partner potentials. That might be the cause of the analysis of fusion observables for heavy systems' startling similarity. It is important to provide numerical evidence for this claim.

Moreover, Eq. (2.1.1) justifies our discussion here, without any doubt, as

$$\sigma_{fus}(E) = \frac{\pi}{k^2}\sum_{\ell}(2\ell+1)\left(1-\left|S_\ell\right|^2\right) \tag{3.3.1}$$

where S_ℓ is the $S-$matrix, which is smoothly related to the corresponding transition probability P_ℓ that can be expressed [1] as in the form of

$$P_\ell = 1-\left|S_\ell\right|^2 = \frac{2\mu}{k\hbar^2}\int_0^\infty dr\, W(r)\left|u(r)\right|^2 \tag{3.3.2}$$

In which is k is the incident wave number $\left(=2\mu E/\hbar^2\right)$, μ and E being the reduced mass and the incident energy in the center of mass frame, respectively. The imaginary part of the nucleus-nucleus potential, $W(r)$ simulates the formation of a compound nucleus by absorbing the incident flux within the Coulomb barrier.

The radial wave function $u_\ell(r)$ in (3.3.2) for the partial wave ℓ is given by [1, 9, and 10]

$$u_\ell(r)=\sqrt{\frac{k}{k_\ell(r)}}T_\ell \exp\left(-i\int_r^{r_{abs}} k_\ell(r')dr'\right) \quad (r\le r_{abs}) \tag{3.3.3}$$

where $k_\ell(r)$ is the local wave number,

$$k_\ell(r)=\sqrt{\frac{2\mu}{\hbar^2}\left(E-U(r)\right)} \quad , \quad U(r)=V_N(r)+V_C(r)+\frac{\ell(\ell+1)}{\hbar^2} \tag{3.3.4}$$

which considers the real part of the full internuclear potential and r_{abs} is the absorption radius, together with $\ell-$ dependent T_ℓ is the transmission coefficient. The primary assumption made here is that the absorption is extremely strong, preventing the incoming flux from rebounding. This is accomplished by setting *W(r)* to a sufficiently large value while neglecting the reflected flux. However in some models, as the ones of interest in this thesis, it is not necessary to explicitly introduce the imaginary component of the inter-nuclear potential. Moreover, the penetration probability, $1-|S_\ell|^2$ in Eq. (3.3.1) can be replaced by $1-|S_\ell|^2=T_\ell$, which offers a significant numerical benefit when dealing with energies that are well below the Coulomb barrier.

Bearing in mind this discussion, in particular Eqn. (3.3.3) and (3.3.4), and also the review of Appendix B that deals with a brief description on the calculation of corresponding radial wave function in coupled channels model, by focusing especially on Esq. (B-4)-(B.6), together with the related discussions in Refs [2,12,13], would make clear the treatment technique of CC calculations for fusion reactions, with the consideration of the whole contributions that come from excited channels. Hence, the whole discussion presented here demonstrates that the usage of

these wave functions, which CC calculations reproduce, reflects the nodal structure in a very weak way, giving results that are similar for the excitation functions in sudden and adiabatic models.

For the final justification of the entire debate here, one may also go back to Fig.3.2 in which the mean angular momentum of the compound nucleus is estimated [9] in a way that

$$\prec \ell \succ (E) = \frac{\frac{\pi}{k^2}\sum_{\ell} \ell\,(2\ell+1)P_{\ell}}{\frac{\pi}{k^2}\sum_{\ell}(2\ell+1)P_{\ell}} \tag{3.3.5}$$

which is the average of fusion cross section (Eq.2.1.1) over $\ell-$values considered during the interaction. Note that Eq. (3.3.1) is transformed to such a partial wave cross section $\sigma_{\ell}(E) = (\pi/k^2)(2\ell+1)T_{\ell}(E)$ leading to $\sigma_{fus}(E) = \sum_{\ell}\sigma_{\ell}(E)$ as in (2.1.1), in which T_{ℓ} is the quantum-mechanical transmission probability through the potential barrier, At this stage it is again emphasized that in all the calculations mentioned in this thesis work, the researchers assumed that incoming flux never bounces back and all is absorbed in the fusion domain which is just beyond/inside the Coulomb barrier.

As the physics behind Fig.3.2 is well discussed in section (3.1), we focus here only the point of interest. With this consideration, one can easily see that the effects of the related terms T_{ℓ} and $U(r)$ in (3.3.3) and (3.3.4) due to the inclusion of different potential function use in sudden and adiabatic models for analysing fusion reactions at low energies is not considerably large. The difference between two models at energies far beyond Coulomb barrier is not due to the potential difference, it might be because of different partial wave (ℓ) consideration. Sudden model uses low partial waves and higher one are cut-off during the calculations due to the shallow potential depth use in the model while the adiabatic model employs both low and higher partial waves all together for the numerical computation of excitation function. Therefore, obtaining the mean angular momentum would be curial when dealing with energies that are below the sub-barrier, which would discriminate explicitly both models. Overall, the potential difference appeared in these treatments

do not cause a striking difference in theoretical reproduction of cross section values at low energies, as shown in Fig.3.3.

For a closing remark, we drawn the attention of the reader to the most recently published [33] an impressive work in which the curvature of the potential barrier, $\hbar w$, has been modified as $\hbar w \to (\hbar w)\exp\left[\lambda \frac{E-V}{V}\right]$ and shown that the modified Wong formula with this incoming term reproduces fusion cross sections pretty well for different systems, involving heavy ion interactions, across the whole energy range including the fusion hindrance phenomena, unlike the original expression. Considering the analysis in [33] one can clearly see that the inadequacy, being the insensitivity of barrier properties such as radius (R), height (V) and curvature $(\hbar w)$ to the angular momentum, in the original Wong formula has been removed through the modification of only the curvature term. The work in [17] thus demonstrates that $\ell-$dependence of R, V and $\hbar w$ may be correlated and can be simulated with a single $\ell-$dependence of the $\hbar w$ term. At this stage, remembering also the $\ell-$ dependency of a shallow phase equivalent partner potential due to elimination of unphysical Pauli forbidden state(s), it is not hard to establish a connection to the shallow nature of the potential behavior in the sudden model because of the same reason: Pauli repulsion between the fermions of reacting nuclei inside the barrier. This sensible connection seems another evidence for justifying the whole discussion in this section.

CONCLUSION

One of the major issues in physics and chemistry is the existence of quantum tunnelling in systems with lots of degrees of freedom. The fusing of two nuclei at extremely low energy is an illustration of a tunnelling phenomenon in nuclear physics. Not only are these reactions crucial for the creation of star energy and nucleosynthesis, but they also shed new light on the reaction dynamics and nuclear structure.

The exploration of fusion hindrance in fusion reactions consist of heavy nuclei at deep sub-barrier energies has recently placed new demands on fusion theory. Therefore, this thesis work has examined in detail the principal advancements in heavy-ion fusion research made over the last 20 years for energies well below the Coulomb barrier. During this time, experimental investigations have extended to these low energies to uncover the unforeseen occurrence of fusion hindrance in such reactions.

Recent studies have shed light on both the reaction's actual mechanism and its dependency on the form and composition of the interacting nuclei. The projected sharp decrease in the cross-section at energies those are deep below the sub-barrier and the creation and improvements of hypotheses to explain this phenomenon are included in the most recent advancements that were summarized in the present review.

We have seen that the standard coupled-channels descriptions need to be improved to take into account the effects of more than one channel, such as nucleon transfer, surface vibrations, and low-lying excitations, and to consider the ion-ion potential as a factor contributing to the hindrance of fusion, which is an important factor in the calculations through the strongly overlapping region. Significant advancements have been achieved with the consideration of a properly constructed short range nucleon-nucleon force to represent the Pauli repulsion between fermions of target and projectile nuclei inside the fusion barrier. Ion-ion potentials with a shallow potential

well and a thicker barrier in the entrance channel potential can sometimes be used to eliminate the apparent discrepancy, according to the calculations related to these inter-nucleon potential functions that were addressed here. This particular example clearly illustrates how the nuclear structure of the nuclei involved in the reaction affects the fusion process.

The greatest prominent impact is the significant enhancement in sub-barrier fusion cross-sections as compared to one-dimensional, single-channel, simple barrier penetration models. Such enhancements can often be clarified by calculations that incorporate coupled channels with couplings to the low-lying surface modes of the interacting nuclei. Determining the number of channels to incorporate and identifying which channels can be safely disregarded are two critical issues in the coupled channels approach. While challenging, this subject has been explored in-depth in the present thesis work, offering some valuable insights. For instance, the excitation of high-lying or giant resonance states can often be neglected as coupling to these states does not impact the shape (or energy dependence) of the calculated fusion cross-section at very deep sub-barrier energies.

The phenomenon of low-energy hindrance is still an active area of research, both experimentally and theoretically. Mişicu and Esbensen proposed a sudden approach using a double folding potential (M3Y+repulsion) that resulted in a shallow pocket due to the incompressibility of nuclear matter. This coupled channels model has effectively replicated hindrance behaviour in various cases. On the other hand, Ichikawa and colleagues suggested adiabatic neck formation between the colliding nuclei in the overlapping region, which leads to hindrance. Their discovery revealed that comprehending fusion hindrance relies significantly on the potential energy at the point of contact, as depicted in Fig.3.4. The incident threshold energies for fusion hindrance show a significant correlation with the touching potential. At incident energies below V_{touch}, the inner turning point of the potential energy occurs inside the contact point. This means that fusion cannot occur until a composite system passes through a residual Coulomb potential with an overlapping configuration. Hence, the dynamics in the overlap region of the two colliding nuclei could cause fusion hindrance.

Furthermore, Simenel et al. [21] proposed a new microscopic model that revealed how the Pauli repulsion effect mainly reduces tunnelling probability within the Coulomb barrier, based on density-constrained frozen Hartree-Fock calculations. It has also been noted that this Pauli blocking effect may be diminished or eliminated in situations where the system has access to positive Q-value transfer channels [25] since several final states can be occupied and valence nucleons can travel between the two nuclei to launch fusion. The claim that Pauli blocking is ineffective (or weakened) in systems with Q > 0 nucleon transfer channels would be seriously questioned in this situation if fusion hindrance were to arise. More specifically, the presence of a number of states after nucleon transfer with Q > 0 effectively balances the Pauli repulsion, which is projected to minimize the probability of tunnelling across the Coulomb barrier. Otherwise, if there are no available channels to transfer positive Q-values, a distinct maximum in the *S*-factor at low energy levels becomes evident, and the logarithmic slope surpasses the L_{CS} value by a significant amount.

We have expanded on previous reviews by offering new insights into the current state of successful theoretical analysis of fusion excitation function measurements across a wide range of energies, including deep sub-barrier levels and discussed the level to which these analyses involving sudden and adiabatic approaches with shallow and deep ion-ion potentials can be explained based on present theories on phase equivalent deep and shallow potential partners within the frame of supersymmetric quantum theory. We anticipate that this concluding discussion will clarify a current argument in the associated literature: How can various analytical treatment models, such as sudden and adiabatic methods, utilizing various ion-ion potential structures with distinctly varied depths, theoretically reproduce cross-section results more similarly? By section (3.3), this question has been explicitly addressed.

As a final remark, the investigation of fusion reactions using radioactive beams is still in its initial phases. The impact of valence nucleons that are weakly bound on the fusion process is not yet well-defined, and additional research is necessary to determine whether the fusion process is enhanced or hindered when utilizing reaction partners with these attributes.

We conclude by pointing out that despite the substantial experimental and theoretical research conducted over the past 20 years on heavy-ion fusion at or below the Coulomb barrier, there are still a number of unanswered questions and issues in this field. The variety of phenomena for which a sufficient theoretical explanation is still lacking serves as evidence of the complexity of heavy-ion fusion dynamics, which is closely related to nuclear structure. It appears that additional experiments will need to be performed in the next years employing sophisticated setups and high-quality exotic beams and extrapolation from prior events; it is also conceivable that unforeseen phenomena and incoming effects may emerge.

REFERENCES

[1] Jiang, C. L.,Back, B. B.,Rehm, K. E., Hagino, K., Montagnoli, G., Stefanini, A. M. (2021). Heavy-ion fusion reactions at extreme sub-barrier energies, The *Eur. Phy. J. A*. **235**, 1-47.

[2] Dasso,C.H.,Landowne, S., Winther, A.(1983).A study of Q-value effects on barrier penetration. *Nucl. Phys. A*.**407**, 221-232.

[3]Jiang, C.L., Esbensen, H., Back, B.B., Janssens, R.V.F., Rehm,K.E.(2004). Analysis of heavy-ion fusion reactions at extreme sub-barrier energies. *Phys. Rev. C* **69**, 014604/1-6.

[4] Beckerman, M. *et al*.(1980). Dynamic Influence of Valence Neutrons upon the Complete Fusion of Massive Nuclei. *Phys. Rev. Lett***. 45**, 1472-1475.

[5] Jiang, C.L. *et al*.(2004).Influence of Nuclear Structure on Sub-Barrier Hindrance in Ni+Ni Fusion. *Phys. Rev. Lett*. **93**, 012701/1-4.

[6] Gönül, B., Özer, O., Yılmaz, M. (2000). Investigation of phase-equivalent potentials by a halo transfer reaction. *Eur. Phys. J. A*.**9**, 19–28.

[7] Hagino, K. (2022). Sub-barrier fusion reactions. *arXiv*:2201.08061v1 [nucl-th] 20 Jan 2022.

[8] Jiang, C. L. and Kay, B. P. (2022). Heavy-ion fusion cross section formula and barrier height distribution. *Phys. Rev*. *C***105**, 064601/1-10.

[9] Balantekin, A. B. and Takigawa, N. (1998). Quantum tunnelling in nuclear fusion. *Rev. Mod. Phys.***70**, 77-100.

[10] Hagino, K. and Takigawa, N. (2012).Subbarrier Fusion Reactions and Many-Particle Quantum Tunnelling. *Prog. Theo. Phys*. **128**, 1061-1106.

[11] Dasgupta, M., Hinde, D. J., Rowley, N. and Stefanini, A.M. (1998). Measuring Barriers to Fusion *Rev. Nucl. Part. Sci*. **48**, 401-461.

[12] Back,B. B.,Esbensen, H., Jiang, C. L., Rehm,K. E. (2014). Recent developments in heavy-ion fusion reactions. *Rev. Mod. Phys.***86**, 317-360.

[13] Montagnoli, G. and Stefanini, A. M. (2017).Recent experimental results in sub- and near-barrier heavy ion fusion reactions. *Eur. Phys. J. A***53,** 169-211.

[14] Wong, C. Y. (1973). Interaction Barrier in Charged-Particle Nuclear Reactions. *Phys. Rev. Lett*. **31**,766-769.

[15] Rowley, N. and Hagino, K. (2015). Examination of fusion cross sections and fusion oscillations with a generalized Wong formula.*Phys. Rev. C* **91**, 044617/1-13.

[16] Jiang,C. L., Esbensen, H, Rehm, K. E.,Back, B. B., Janssens, R.V.F., Caggiano, J. A.,Collon, P., Greene, J., Heinz, A. M., Henderson, D. J.,Nishinaka, I., Pennington, T. O., and Seweryniak, D. (2002). Unexpected Behavior of Heavy-Ion Fusion Cross Sections at Extreme Sub-Barrier Energies. *Phys. Rev. Lett.* **89**, 052701/1-4.

[17] Mişicu, S. (2014). An inquiry on hindrance to heavy-ion sub-barrier fusion. *Int. J. Mod. Phys. E***23**, 1450074/1-37.

[18]Mişicu,Ş. and Esbensen, H.(2006). Hindrance of Heavy-Ion Fusion due to Nuclear Incompressibility. *Phys. Rev. Lett.***96**, 112701/1-4.

[19]Mişicu, Ş. and Esbensen, H. (2007). Signature of shallow potentials in deep sub-barrier fusion reactions. *Phys. Rev. C***75**, 034606/1-14.

[20] Bertsch, G., Borysowicz,W., McManus, H. and Love, W. G. (1977). Interactions for inelastic scattering derived from realistic potentials. *Nucl. Phys. A***284**, 399-419.

[21] Simenel, C., Umar, A. S., Godbey, K., Dasgupta, M. and Hinde, D. J. (2017). How the Pauli exclusion principle affects fusion of atomic nuclei. *Phys. Rev. C***95**, 031601(R)/1-6.

[22] Esbensen, H., Wu, J.-Q. and Bertsch, G. F. (1983). Subbarrier Fusion and Dynamical Deformations. *Nucl. Phys. A***411**, 275-288.

[23] Ichikawa, T., Hagino, K. and Iwamoto, A.(2007).Existence of a one-body barrier revealed in deep subbarrier fusion. *Phys. Rev. C***75**, 057603/1-4.

[24] Ichikawa, T. (2015). Systematic investigations of deep sub-barrier fusion reactions using an adiabatic approach. *Phys. Rev. C***92**, 064604/1-19.

[25] Esbensen, H. and Stefanini, A. M. (2014). Influence of multiphonon excitations and transfer on the fusion of Ca+Zr. *Phys. Rev. C***89**, 044616/1-15.

[26] Cheng K. X. and Xu, C. (2019). Pauli blocking effects in α-induced fusion reactions. *Phys. Rev. C***99**, 014607/1-7.

[27]Cheng, K. X. and Xu, C. (2020). Pauli blocking effects in nα-nucleus-induced fusion reactions. *Phys. Rev. C* 102, 014619/1-7.

[28]Cheng K. X., Xu, C., Ma, C.W., Pu, J., Wang, Y.T. (2022). Pauli blocking potential applied to heavy-ion fusion reactions. *Chin. Phys. C***46**, 024105/1-9.

[29] Dasso, C.H., Pollarolo, G.(2003). Investigating the nucleus-nucleus potential at very short distances. *Phys. Rev. C***68**, 054604/1-3.

[30] Ohkubo, S. (2017). Luneburg-lens-like structural Pauli attractive core of the nuclear force at short distances. *Phys. Rev. C* **95**, 044002/1-6.

[31] Baye, D. (1987). Supersymmetry between Deep and Shallow Nucleus-Nucleus Potentials. *Phys. Rev. Lett*. **58**, 2738-2741.

[32]Sparenberg,J.-M. and Baye,D. (1997). Supersymmetry between Phase-Equivalent Coupled-Channel Potentials. *Phys. Rev. Lett*. **79**, 3802-3805.

[33] Jiang, C.L. (2022). A modified Wong formula for heavy-ion reactions. *Eur. Phys. J. A***72**, 1-8.

APPENDIX A
THE ION-ION POTENTIAL

This section deals with the form of interaction potential between heavy-ions in the light of Ref. [12]. A crucial component of calculations involving coupled-channels is the ion-ion potential $U(r)$. It determines both the nuclear couplings to the excited states of the interacting nuclei and the height of the Coulomb barrier. The ion-ion potentials that have been used are often of the Woods- Saxon type

$$U(r) = \frac{U_0}{1+\exp\left[(r-R)/a\right]} \tag{A.1}$$

where U_0 is the depth, R is the radius of the nucleus, and a is the diffuseness of the potential. Standard set of parameters that are consistent with the analysis of elastic scattering data can be found in any textbook concerning with nuclear physics. The empirical potential is a smooth function of the mass numbers of the reacting nuclei and may need small adjustments, for example, of the depth U_0 or the radius R, in order to optimize the fit to fusion data. After appearance of fusion hindrance problem in the literature, researchers soon realized that the Woods-Saxon parameterization of the ion-ion potential is unrealistic for overlapping nuclei and provides a poor description of the fusion data at extreme sub-barrier energies. See for instance Section III of Ref. [12]. One way to overcome this problem is to use a double-folding potential and adjust it for overlapping nuclei so that it provides a better description at very low energies. The potential is given by

$$U(r) = \int dr_1 \int dr_2 \, \rho_1(r_1)\rho_2(r_2)v_{n-n}(r+r_2-r_1) \tag{A.2}$$

where $\rho_{1,2}$ are the densities of the reacting nuclei and v_{n-n} is a short ranged nucleon-nucleon interaction. An interaction that is often used is the M3Y interaction which was introduced by Bertsch and his collaborators [20]. This interaction produces an ion-ion potential outside the barrier region that is in good agreement with the empirical Woods-Saxon potential for elastic scattering discussed in [12]. It was

proven quite reliable in predicting the height of the Coulomb barrier [19].Because it is substantially deeper than the ground-state energy of the compound nucleus, the predicted entrance channel potential for overlapping nuclei is implausible. The effective n-n interaction should therefore be supplemented with a repulsive contact term which is calculated by inserting the interaction into the double-folding expression in (A.2). The diffuseness and strength of the potential is adjusted to optimize the fit of coupled-channels calculations to the fusion data [18].The total ion-ion potential is referred to as the M3Y + repulsion potential. The radii (R) of the reacting nuclei and the diffuseness (a), which controls the depth of the pocket in the entrance channel potential, are fundamentally the two types of adjustable parameters in this potential. The effects of repulsive n-n interaction through ion-ion potential, involving nuclear and Coulomb interactions, was already illustrated through Figs. (2.3) , (2.5) and (2.6). In addition to these illustrations, further examples of entrance channel potentials for the fusion of ^{48}Ca +^{48}Ca are shown below in Fig.A.1, which is taken from Ref. [12]. Obviously, the best representation of experimental observation through theoretical calculations is achieved by M3Y + repulsion potential when compared to M3Y and Woods-Saxon potentials. This clarifies the requirement for the consideration of a physically plausible repulsive potential function within the frame of inter-nucleon interactions in the inner region of the barrier. This additional consideration in reality mimics the Pauli repulsion between the quarks of neutrons and protons in compound nucleus during the fusion case.

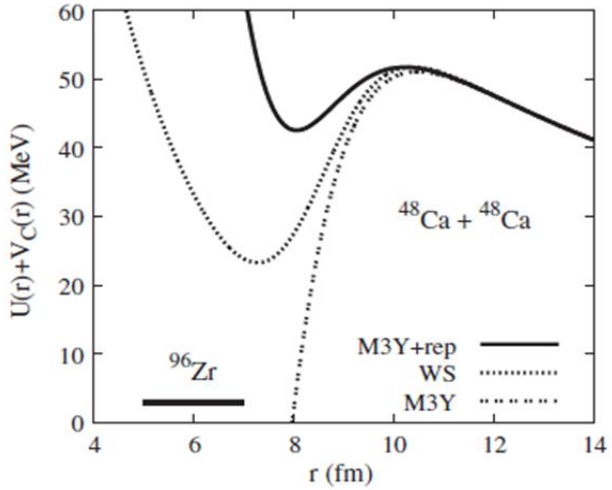

Fig.A.1 Entrance channel potentials for the fusion of $^{48}Ca + ^{48}Ca$. The Woods-Saxon potential (dotted curve) is compared to the M3Y potential with (solid curve) and without (dashed curve) repulsion. The corresponding ground-state energy of the fused system ^{96}Zr is also indicated by the horizontal bar. Taken from [12].

In summary, the identification of the fusion hindrance phenomenon sparked a broad debate concerning the underlying physics. The shape of the nuclear potential on the inner side of the Coulomb barrier affects the deep sub-barrier fusion cross sections for heavy nuclei interactions; it has been noted throughout the study described in this thesis. Thus, one can look into the radial dependency of the ion-ion potential at extremely close distances using the findings of those measurements made far below the barrier .From a phenomenological perspective, the experimental results show that, in comparison to the often employed standard potentials, a thicker and shallower barrier is needed, like W-S and M3Y potentials. Mişicu and Esbensen [18, 19] showed that the incompressibility of nuclear matter may lead to a repulsive core in the potential at short distances, which is discussed in sections (2.2.1) and (2.2.2), due to Pauli repulsion effect between the quarks of target and projectile nuclei.

As a result, they suggested using the double folding potential M3Y in the ion-ion interaction with an additional repulsive core (M3Y + repulsion), which does form a shallow pocket inside the Coulomb barrier. In several of the examples addressed throughout the current work in this thesis, the hindrance phenomenon has been rather successfully reproduced by employing this sudden approach using the M3Y + repulsion potential.

APPENDIX B

A BREIF DICUSSION ABOUT COUPLED-CHANNELS EQUATIONS

The modelling of the proper Hamiltonian and the identification of relevant degrees of freedom are essential components of the coupled-channels calculations. The initial calculations for heavy-ion fusion using coupled channels made an assumption on the linear coupling to quadrupole or octupole surface vibrations and quadrupole deformations. The significance of the hexadecapole deformations, neutron transfer, coupling of multiphonon states, and higher-order couplings was revealed as more precise data became available. Here below we briefly illustrate the basic principles and the framework of the CC model, in the limit where the incident energy is large compared to the excitation energies of the relevant coupled states and to the coupling interaction. This is usually called the sudden limit.

Within this frame, the nuclear structure effects can be taken into account in a more quantal way [9,10, 13] using the coupled-channels method. In order to formulate the coupled-channels method, consider a collision between two nuclei in the presence of the coupling of the relative motion (r) to a nuclear intrinsic motion ξ. In this case one assumes, in a simple manner, the following Hamiltonian for this system,

$$H(r,\xi) = -\frac{\hbar^2}{2\mu}\nabla^2 + U(r) + H_0(\xi) + V_{coup}(r,\xi) \qquad \text{(B.1)}$$

Where $U(r)$ is the ion-ion potential (with nuclear and Coulomb interactions) while $H_0(\xi)$ and $V_{coup}(r,\xi)$ are the intrinsic and the coupling Hamiltonians, respectively.

The intrinsic motion wavefunction is described as

$$H_0(\xi)\varphi_n(\xi) = \varepsilon_n \varphi_n(\xi) \qquad \text{(B.2)}$$

Where ε_n is the excitation energy of *nth* channel. By introducing the eigenstates φ_n of H_0 and by expanding the total wave function in terms of those eigenstates, that is

$$\Psi(r,\xi)=\sum_n u_n(r)\varphi_n(\xi) \tag{B.3}$$

The stationary Schrödinger equation is equivalent to the set of coupled equations for the wave functions u_n of the relative motion

$$\left[-\frac{\hbar^2}{2\mu}\frac{d^2}{dr^2}+U(r)+\frac{\ell_n(\ell_n+1)\hbar^2}{2\mu r^2}-E\right]u_n(r)=-\sum_m\left[\varepsilon_n\delta_{nm}+\langle\varphi_n|V_{coup}(r,\xi)|\varphi_m\rangle\right]u_m(r) \tag{B.4}$$

One may impose the usual boundary conditions for a scattering problem and consider the case where the coupling interaction can be factorised as follows

$$\langle\varphi_n|V_{coup}(r,\xi)|\varphi_m\rangle=F(r)\langle\varphi_n|G(\xi)|\varphi_m\rangle=F(r)G_{nm} \tag{B.5}$$

Where $F(r)$ is the form factor associated to the relative motion and G_{nm} only depends on the intrinsic variables describing nuclear structure. So we can write

$$\left[-\frac{\hbar^2}{2\mu}\frac{d^2}{dr^2}+U(r)+\frac{\ell_n(\ell_n+1)\hbar^2}{2\mu r^2}-E\right]u_n(r)=-\sum_m M_{nm}u_m(r) \tag{B.6}$$

Where

$$M_{nm}=\varepsilon_n\delta_{nm}+F(r)G_{nm} \tag{B.7}$$

For the more complex vibrational and rotational collective low-lying state consideration, together with the codes used for the computation of CC calculations, the reader is referred to Ref [9, 10, and 13] and the other related references therein. With such high accuracy, it has been possible to explain how sub-barrier fusion processes work in terms of quantum tunnelling of systems with many degrees of freedom. In particular Figs.2.4, 2.7, 2.8, and 2.9 have previously transparently clarified the effects of the coupling of the relative motion between the target and projectile nuclei to their intrinsic excitations.

Furthermore, the recent CC analysis, discussed in Ref. [13], of the excitation function is illustrated below. It includes explicitly one- and two nucleon transfer channels, in addition to inelastic channels, with coupling strengths calibrated to reproduce the measured neutron transfer data. Such transfer couplings bring significant cross section enhancements, even at the level of a few μb.

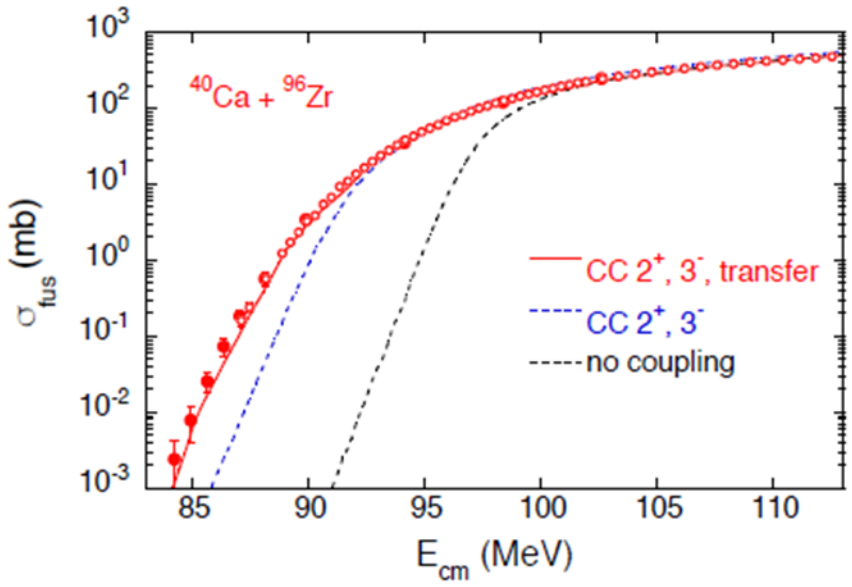

Fig.B.1 Fusion cross sections for ^{40}Ca + ^{96}Zr are compared with CC calculations (taken from Ref.[13]). The red line reproducing the data includes couplings to the one- and two-nucleon transfer channels besides the inelastic excitation 2^+ and 3^- of both nuclei.

APPENDIX C

POTENTIAL DESCRIPTION IN THE ADIABATIC APPROACH

In the light of Refs. [23,24],we describe below an extension of the standard CC framework following the strategy mentioned in the adibatic model discussed in Section (3.1). To this end, we introduce the damping factor $\Phi\left(r,\lambda_\alpha\right)$ for the nucleus-nucleus coupling interaction potential with respect to the eigenchannel α,

$$V_N\left(r,\lambda_\alpha\right)=V_N^0\left(r\right)+\left[-\frac{dV_N^0}{dr}\lambda_\alpha+\frac{d^2V_N^0}{dr^2}\lambda^2\right]\Phi\left(r,\alpha\right) \qquad \text{(C.1)}$$

The addition of the damping factor within the frame of the adiabatic approach is the most significant modification to the standard CC treatment. The physical process of gradually moving from sudden to adiabatic approximations is represented by this damping factor, which reduces the excitation strengths of the target and/or projectile vibrational states after the two colliding nuclei overlap.To describe it, authors of [23,24] suggested to choose the damping factor as in the form of

$$\Phi\left(r.\alpha\right)=e\exp\left(r-R_d-\lambda_\alpha\right)^2/2a_d^2 \quad , \quad r\prec R_d+\lambda_\alpha \quad \text{(overlapping region)} \qquad \text{(C.2)}$$

otherwise $\Phi\left(r,\lambda_\alpha\right)=1$ that describes two-body region. In Eq. (C.2), the term $R_d\left(=r_d\left(A_p^{1/3}+A_t^{1/3}\right)\right)$is the spherical touching distance between the target and the projectile, as shown in Fig. (3.4), together with r_d and a_d being with and ad are the damping radius and diffuseness parameters respectively.An important point of these modifications is that the touching point in the damping factor depends on λ_α which implies that the excitation strength begins to reduce at different distances in each eigenchannell during the reaction. For the details of such calculations, the reader is refered to [23,24].

CURRICULUM VITAE

Personal information:

Name: Hatice ŞABRAK

Languages:

- Very good at speaking and writing in English.
- Good speaking and writing in Turkish.
- Native language: Arabic.

Education:

- Bachelor's degree in engineering physics
- Master’s degree in nuclear physics

  From GAZIANTEP University-faculty of Engineering–Gaziantep TÜRKİYE.